

Online Supplement

Chymotrypsin-like Elastase-1 Mediates Progressive Emphysema in Alpha-1 Antitrypsin Deficiency

Andrew J. Devine, BS*¹ Noah J. Smith, BS*² Rashika Joshi, MD¹ Qiang Fan, PhD¹ Michael T. Borchers, PhD^{1,3} Jeremy C. Clair, PhD⁴ Joshua N. Adkins, PhD⁴ Brian M. Varisco, MD^{1,2}

¹ Division of Critical Care Medicine, Cincinnati Children's Hospital Medical Center, Cincinnati, Ohio, United States

² University of Cincinnati School of Medicine, Cincinnati, Ohio, United States

³ Division of Pulmonary and Critical Care Medicine, University of Cincinnati, Cincinnati, Ohio, United States

⁴ Pacific Northwest National Laboratory, Richland, Washington, United States

* *Authors contributed equally*

Supplemental Table 1: Genes 2-fold increased or decreased protein abundance in AAT-deficient vs wildtype lungs

Two-fold reduced in AAT-deficient compared to wildtype	adjusted p-value	log(AAT/WT)	Two-fold increased in AAT-deficient compared to wildtype	adjusted p-value	log(AAT/WT)
Alpha-1-antitrypsin 1-4	0.005402969	-7.658939793	Very-long-chain (3R)-3-hydroxyacyl-CoA dehydratase 2	0.635451325	4.356620473
Alpha-1-antitrypsin 1-1	0.104629553	-4.127926977	Septin-5	0.814392232	2.569137722
Alpha-1-antitrypsin 1-2	0.24021247	-3.840431444	Mannose-6-phosphate isomerase	0.814392232	2.40962705
CapZ-interacting protein	0.76976043	-2.962319502	Endoplasmic reticulum metallopeptidase 1	0.706555434	2.202271146
Phosphatidylinositol 5-phosphate 4-kinase type-2 alpha	0.710098202	-2.818698064	SLC-ROBO Rho GTPase-activating protein 2	0.814392232	2.155599029
Ubiquinone biosynthesis monooxygenase COQ6, mitochondrial	0.548562953	-2.526899803	Carboxypeptidase Q	0.814392232	2.118892851
USP6 N-terminal-like protein	0.76976043	-2.320869555	Golgin subfamily A member 2	0.814392232	2.110520803
Geranylgeranyl pyrophosphate synthase	0.635451325	-2.241314546	Collagen alpha-2(V) chain	0.814392232	2.050161614
Histone H2A type 1-F	0.710098202	-1.869754004	Plasma kallikrein	0.814392232	2.037018714
Nuclear autoantigen Sp-100	0.716466787	-1.680303091	Transmembrane protein 256	0.787335326	1.999844798
CD99 antigen	0.706555434	-1.256946612	Ubiquitin-like domain-containing CTD phosphatase 1	0.814392232	1.983197913
[Pyruvate dehydrogenase (acetyl-transferring)] kinase isozyme 2,	0.76976043	-1.215477898	Active breakpoint cluster region-related protein	0.710098202	1.964948073
Non-histone chromosomal protein HMGB-14	0.76976043	-1.201008833	Zinc finger and BTB domain-containing protein 20	0.836830423	1.922906569
Ras-specific guanine nucleotide-releasing factor 2	0.76976043	-1.167508425	Matrix metalloproteinase-9	0.814392232	1.899151387
cAMP-dependent protein kinase type II-beta regulatory subunit	0.670739978	-1.100712009	Gamma-interferon-inducible lysosomal thiol reductase	0.814392232	1.84450418
Ig heavy chain V region AC38 205.12	0.772417645	-1.055441928	Serum amyloid A-4 protein	0.814392232	1.79859424
Enhancer of rudimentary homolog	0.635451325	-1.036661021	Complement C2	0.710098202	1.791135782
			Prefoldin subunit 3	0.799651701	1.76560095
			Alpha-1-acid glycoprotein 1	0.786781732	1.746757615
			Dynein light chain Tctex-type 3	0.799651701	1.653570064
			Secretory carrier-associated membrane protein 1	0.836830423	1.631691006
			SH3 domain-containing kinase-binding protein 1	0.799651701	1.626019142
			Mitochondrial import receptor subunit TOM40 homolog	0.814392232	1.601646268
			Cytoplasmic dynein 2 heavy chain 1	0.793717161	1.597597047
			IST1 homolog	0.814392232	1.587979889
			Plakophilin-2	0.706555434	1.575039769
			Aldehyde oxidase 1	0.814392232	1.517322151
			Double-strand-break repair protein rad21 homolog	0.836830423	1.506272632
			Disks large-associated protein 4	0.814392232	1.476735135
			RNA helicase aquarius	0.799651701	1.460264526
			AP-1 complex subunit mu-2	0.836830423	1.363440153
			Centrin-2	0.799651701	1.359339453
			Epidermal growth factor receptor	0.832446546	1.358962695
			Conserved oligomeric Golgi complex subunit 1	0.814392232	1.348375208
			Volume-regulated anion channel subunit LRRC8C	0.814392232	1.330912411
			Bola-like protein 2	0.814392232	1.316034624
			Bifunctional epoxide hydrolase 2	0.814392232	1.315689693
			C-type lectin domain family 11 member A	0.706555434	1.284167018
			DnaJ homolog subfamily B member 11	0.836830423	1.279985812
			Actin-related protein 2/3 complex subunit 5-like protein	0.814392232	1.272532949
			Transmembrane protein 214	0.799651701	1.25521081
			Retinoid-inducible serine carboxypeptidase	0.814979184	1.253613023
			H-2 class II histocompatibility antigen gamma chain	0.814392232	1.250222229
			Protein AMBP	0.848218401	1.24815933
			Collagen alpha-1(VIII) chain	0.814392232	1.243450557
			Ragulator complex protein LAMTOR5	0.841242473	1.234339674
			Interferon-induced helicase C domain-containing protein 1	0.814392232	1.228872136
			WD repeat-containing protein 82	0.814392232	1.208879749
			E3 ubiquitin-protein ligase HECTD1	0.814392232	1.205309685
			Serine protease 56	0.821064821	1.197847018
			AH receptor-interacting protein	0.832446546	1.197386863
			Haptoglobin	0.76976043	1.188611838
			U6 snRNA-associated Sm-like protein Lsm2	0.814392232	1.168714164
			Neutrophil gelatinase-associated lipocalin	0.814392232	1.152929464
			Charged multivesicular body protein 2a	0.799651701	1.146736093
			GTP-binding protein Rit1	0.849719788	1.140625331
			Polyprenol reductase	0.814392232	1.139162093
			Integrin alpha-M	0.814392232	1.111257911
			Bromodomain-containing protein 4;Bromodomain-containing protein 3	0.814392232	1.094684836

Supplemental Table 2: Genes 2-fold increased or decreased protein abundance in Cela1&AAT-deficient vs AAT-deficient lungs

<u>Two-fold decreased in Cela1&AAT-deficient compared to AAT-deficient</u>	adjusted	p-value	log(DKO/AAT)	<u>Two-fold increased in Cela1&AAT-deficient compared to AAT-deficient</u>	adjusted	p-value	log(DKO/AAT)
Very-long-chain (3R)-3-hydroxyacyl-CoA dehydratase 2	0.635451325		-4.356620473	USP6 N-terminal-like protein	0.76976043		2.320869555
Septin-5	0.814392232		-2.569137722	RNA-binding motif protein, X chromosome	0.814392232		2.28054377
Mannose-6-phosphate isomerase	0.814392232		-2.409962705	Geranylgeranyl pyrophosphate synthase	0.635451325		2.241314546
Zinc finger and BTB domain-containing protein 20	0.836830423		-1.922906569	Septin-10	0.814392232		2.1716133508
Matrix metalloproteinase-9	0.814392232		-1.899151387	Polyadenylate-binding protein 2	0.814392232		1.76735785
Serum amyloid A-4 protein	0.814392232		-1.79859424	Protein phosphatase 1 regulatory subunit 12B	0.814392232		1.757948104
Prefoldin subunit 3	0.799651701		-1.76560095	Homer protein homolog 3	0.814392232		1.751469843
Alpha-1-acid glycoprotein 1	0.786781732		-1.746757615	PRKC apoptosis WT1 regulator protein	0.814392232		1.624204285
Plakophilin-2	0.706555434		-1.575039769	E3 ubiquitin-protein ligase Itchy	0.814392232		1.606612821
Double-strand-break repair protein rad21 homolog	0.836830423		-1.506272632	Alpha-1,3/1,6-mannosyltransferase ALG2	0.814392232		1.592098663
Disk large-associated protein 4	0.814392232		-1.476735135	Nostrin	0.814392232		1.580235527
Bola-like protein 2	0.814392232		-1.316034624	NHP2-like protein 1	0.814392232		1.535833642
C-type lectin domain family 11 member A	0.706555434		-1.284167018	ER membrane protein complex subunit 7	0.814392232		1.534010735
Actin-related protein 2/3 complex subunit 5-like protein	0.814392232		-1.272532949	Dynactin subunit 3	0.836830423		1.481142994
Serine protease 56	0.821064821		-1.197847018	Equilibrative nucleobase transporter 1	0.814392232		1.443035311
U6 snRNA-associated Sm-like protein LSm2	0.814392232		-1.168714164	60S ribosomal protein L36	0.816225412		1.425669401
Bromodomain-containing protein 4;Bromodomain-containing protein 3	0.814392232		-1.094684836	LIM and cysteine-rich domains protein 1	0.814392232		1.398942749
Vacuolar protein sorting-associated protein VTA1 homolog	0.835350159		-0.966865802	Sphingosine-1-phosphate lyase 1	0.814392232		1.377943636
Tumor protein p63-regulated gene 1-like protein	0.814392232		-0.963464717	Palmdelphin	0.814392232		1.365293779
				Cytoglobin	0.814392232		1.280099477
				Serine protease HTRA2, mitochondrial	0.821183794		1.219441125
				Vacuolar protein sorting-associated protein 33A	0.847893608		1.215416973
				Oxidation resistance protein 1	0.814392232		1.194977614
				PTB domain-containing engulfment adapter protein 1	0.836830423		1.068995294
				Ig heavy chain V region AC38 205.12; Ig heavy chain V region J558; Ig heavy chain V region MO	0.772417645		1.055441928
				Calcineurin B homologous protein 1	0.836830423		1.053178882
				TIP41-like protein	0.836830423		1.04728927
				Malectin	0.833615817		0.981350537

Supplemental Figure Titles and Legends

Figure S1: Titration in Lipopolysaccharide Model of AAT-deficient Emphysema. (A) Middle lobe sections of AAT-deficient mice treated with PBS (B) 1 unit of LPS at day 1 and 0.5 units at day 10 (C) 2 and 1 units, (D) 5 & 2.5 units, and (E) 10 & 5 units. (F) Middle lobes of wildtype (WT) mice treated with 10 & 5 units of LPS. (G) Airspace diameter percentile values of tile scanned lung lobe sections of the mice above showing that emphysema was no worse in *AAT*-deficient mice than WT.

Figure S2: Titration of tracheal PPE in *AAT*-deficient Mice. Tile scanned images of *AAT*-deficient (AAT) and wildtype (WT) mice 21 days after different doses of porcine pancreatic elastase (PPE). AAT mice had evidence of substantial emphysema at the lowest tested dose (0.25 units).

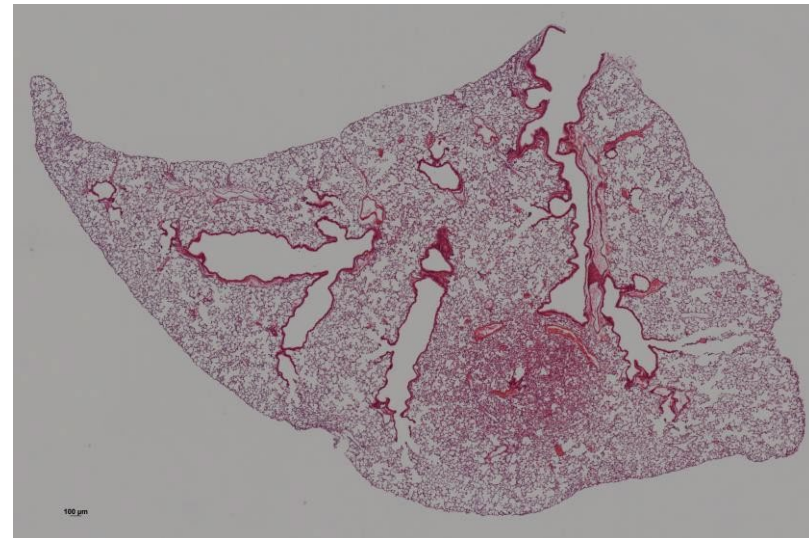
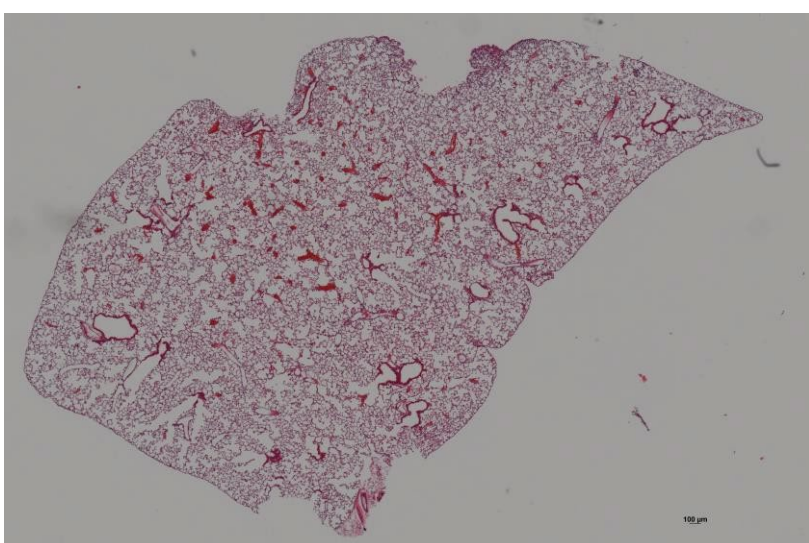
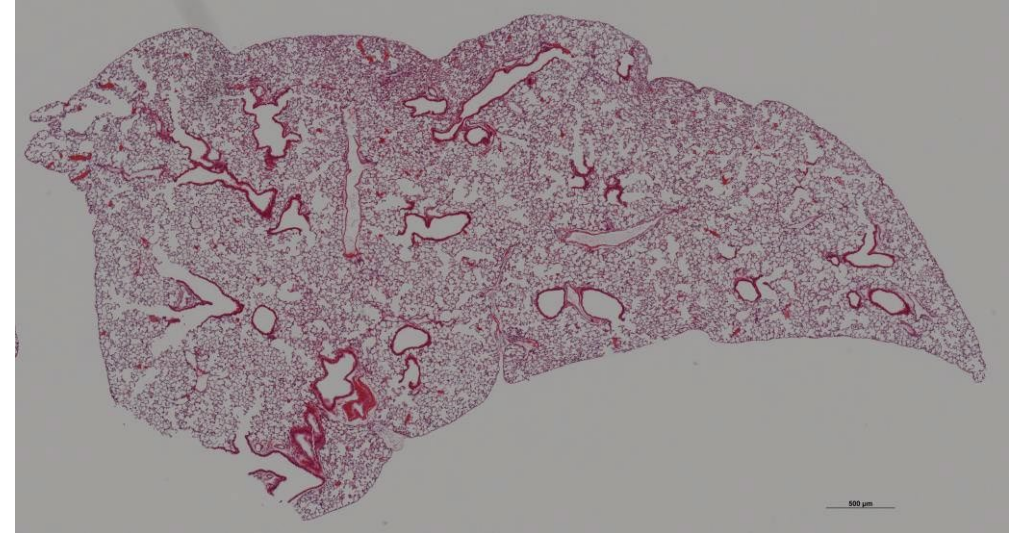
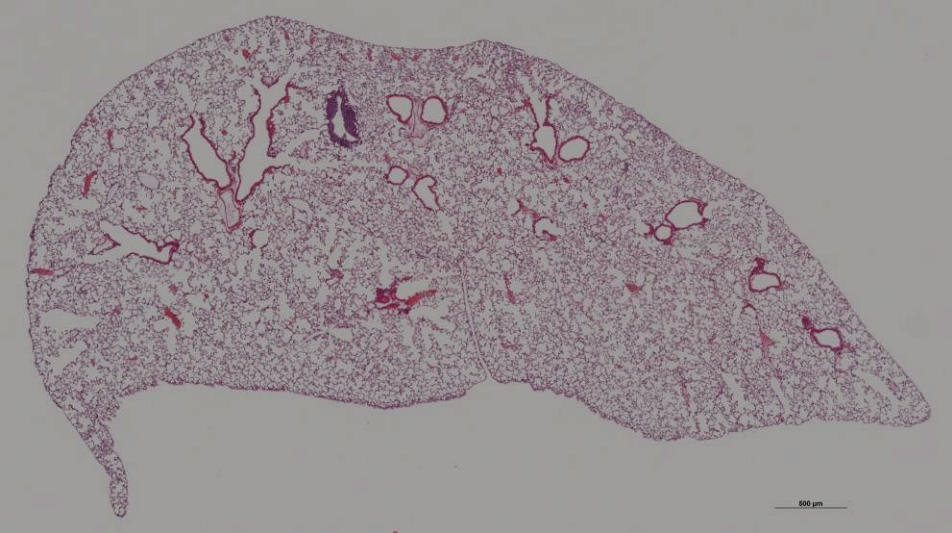
Figure S3: Complete Protein-protein Interaction Network for *AAT*^{-/-} vs wildtype mice. The complete protein-protein interaction network of proteins with significantly different abundance between *AAT*-deficient and wildtype mouse lungs 42 days after low-dose tracheal PPE.

Figure S4: Complete Protein-protein Interaction Network for *AAT*^{-/-}&*Cela1*^{-/-} mice vs *AAT*^{-/-} mice. The complete protein-protein interaction network of proteins with significantly different abundance between *AAT*^{-/-}&*Cela1*^{-/-} vs *AAT*^{-/-} mouse lungs 42 days after low-dose tracheal PPE.

Supplemental Figure 1

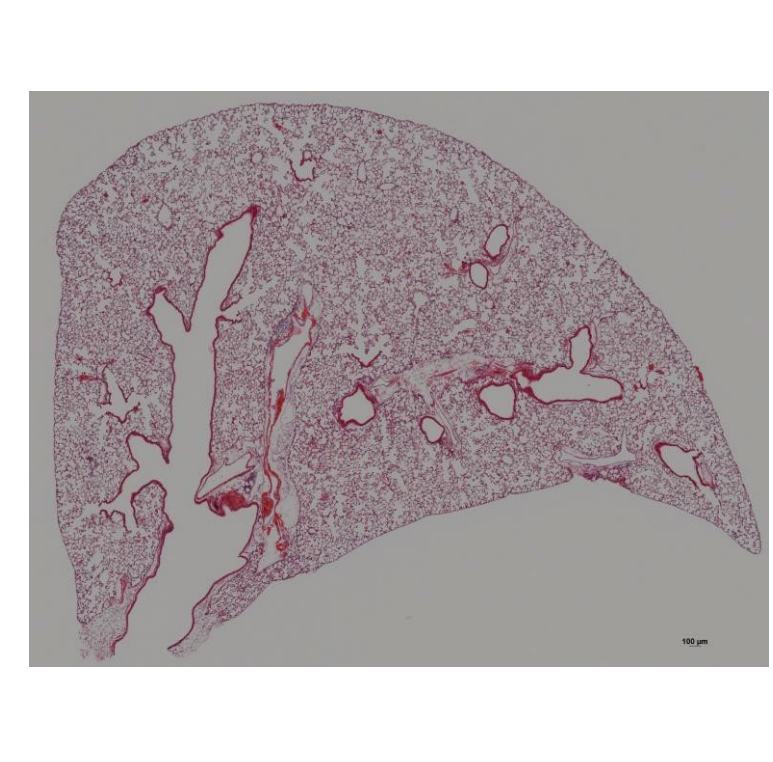
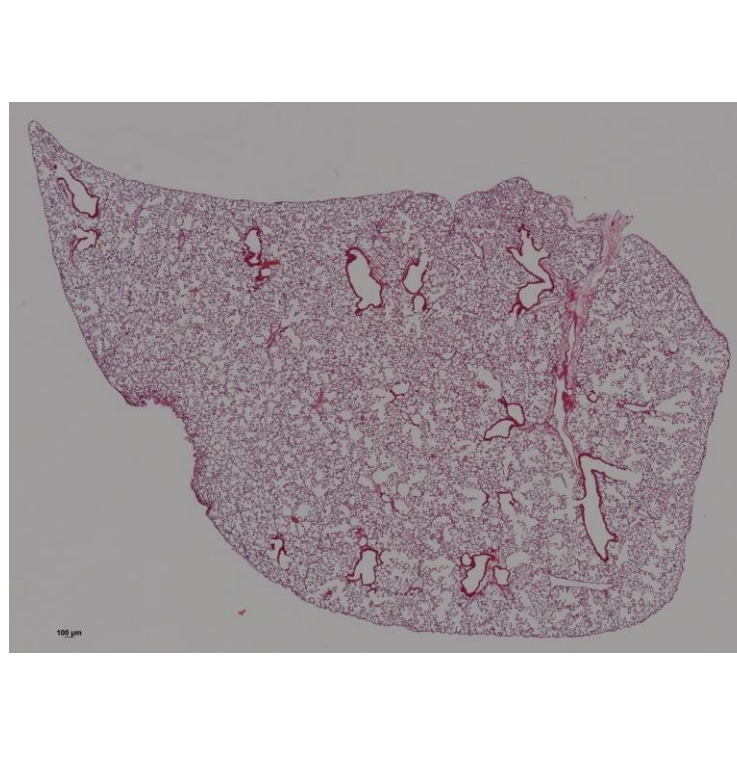
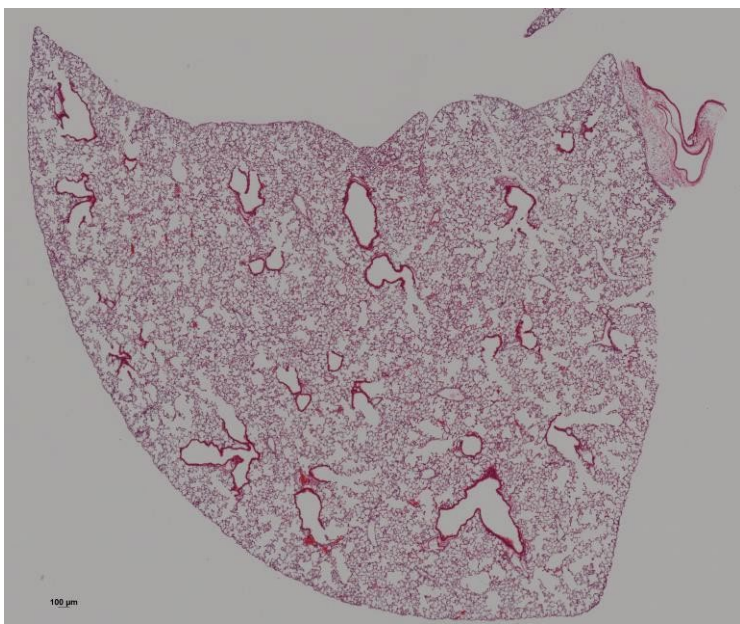
AAT KO PBS

A

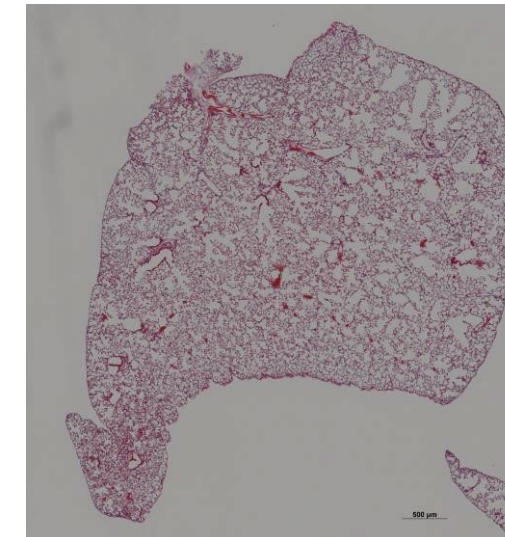
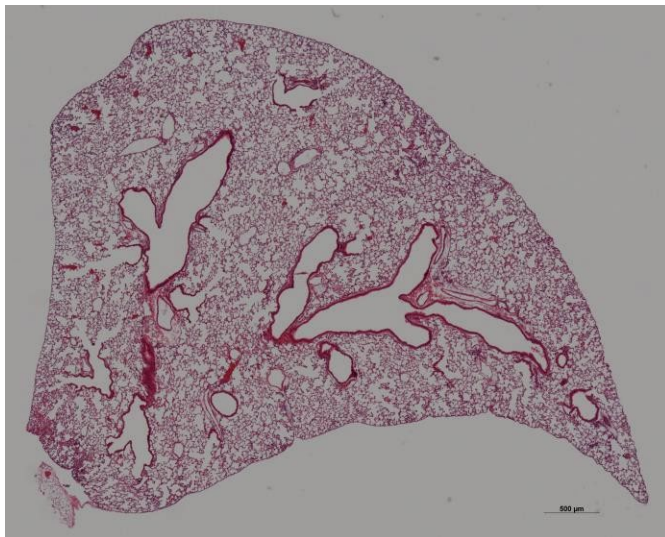
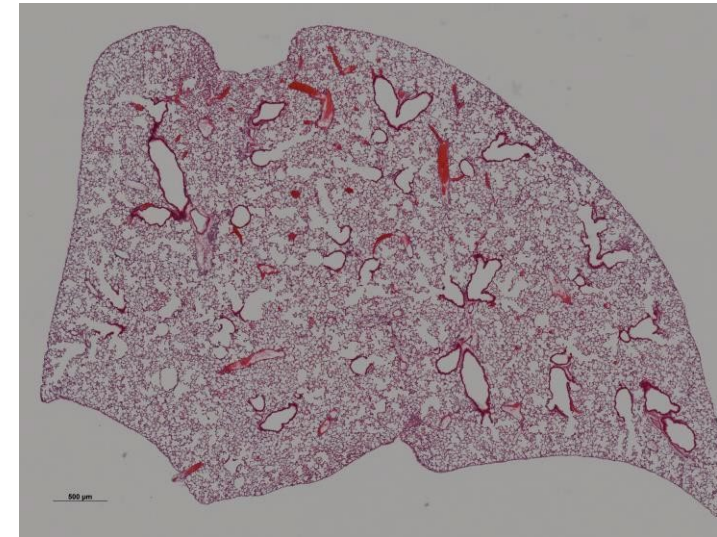
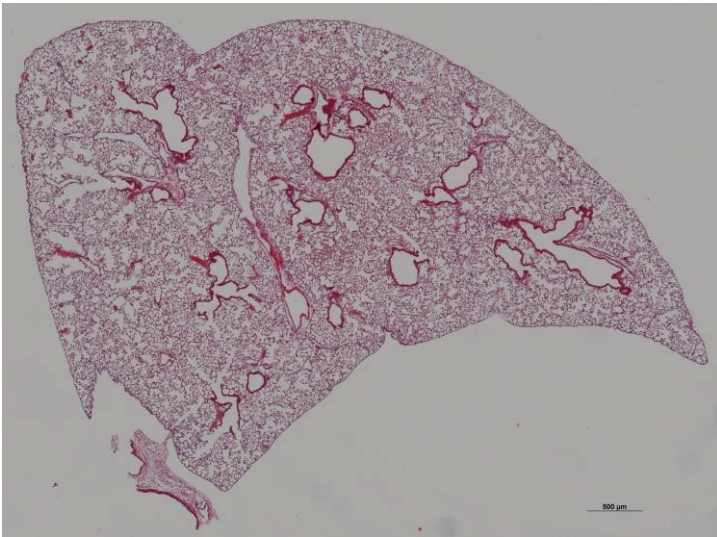


WT 21 days 1&0.5 Units LPS

B

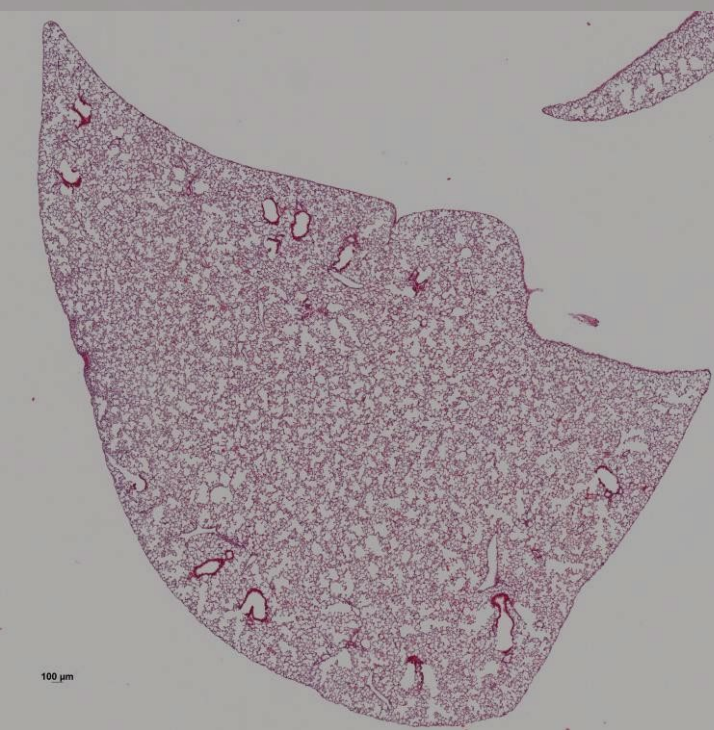
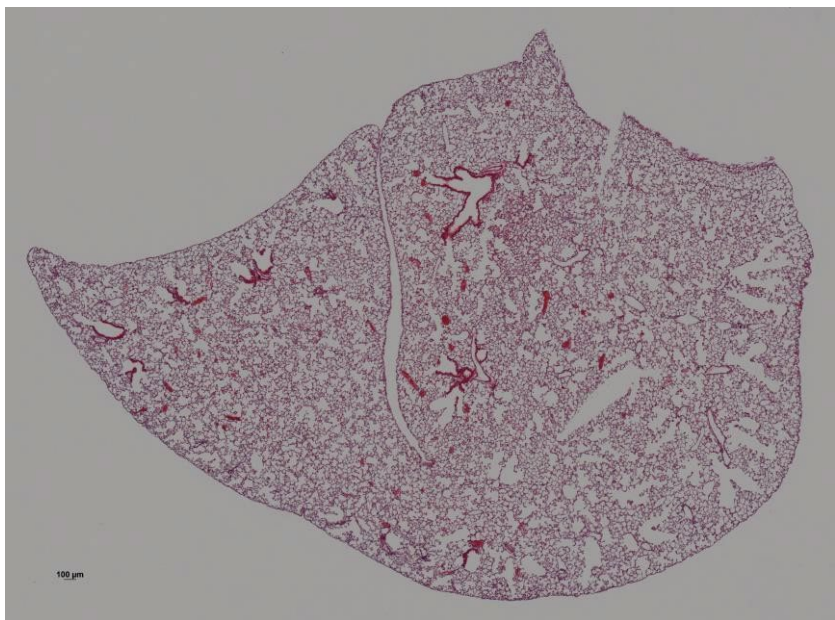
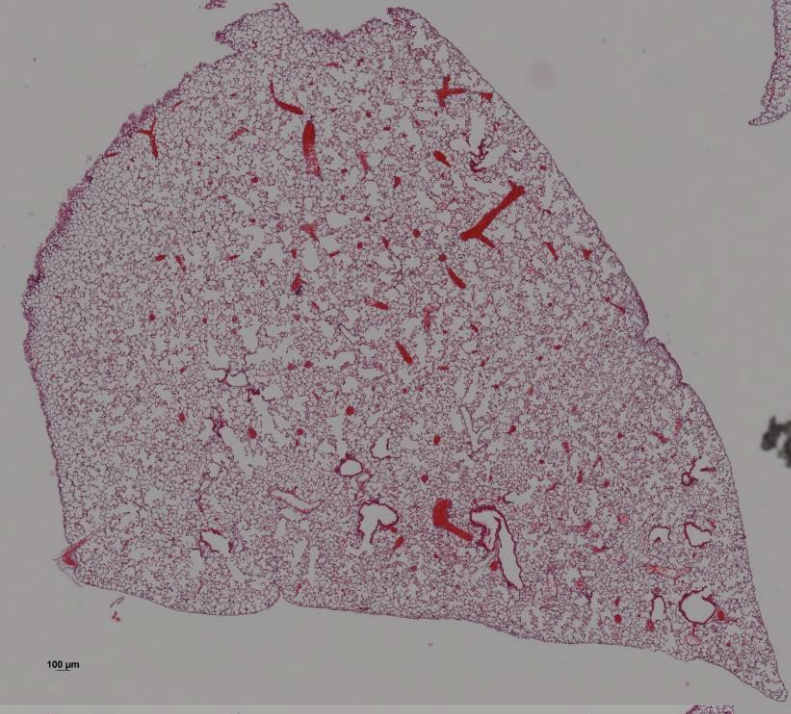
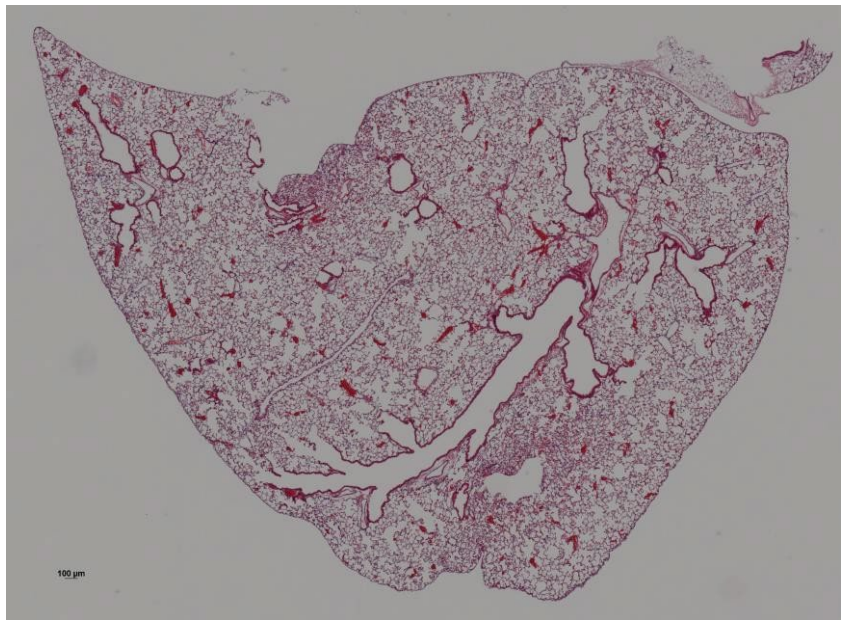


AAT KO 21 days 1&0.5 Units LPS



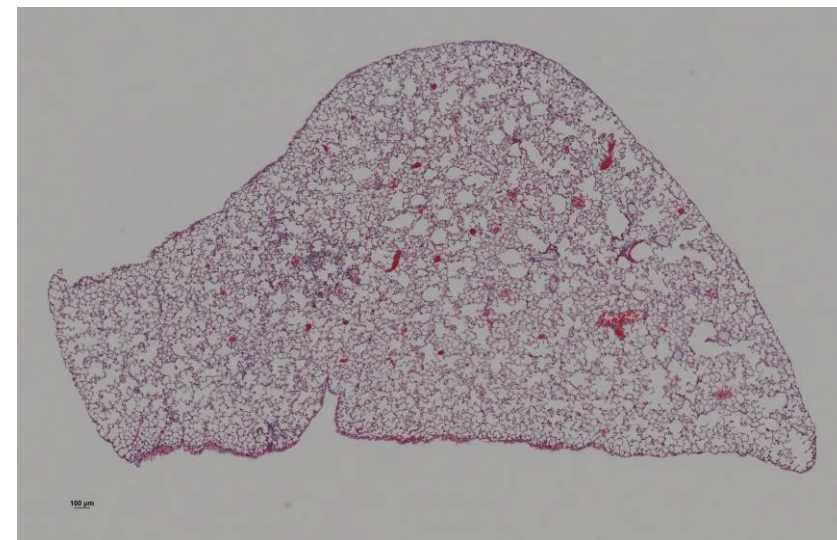
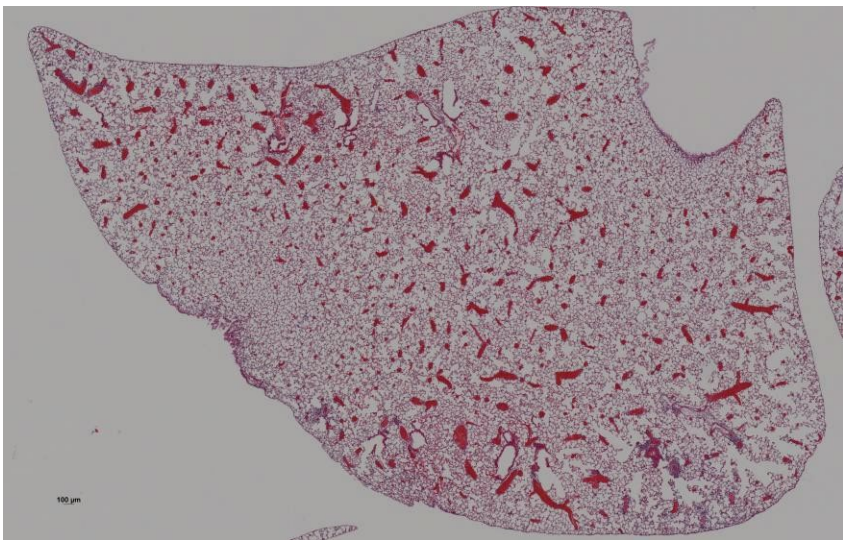
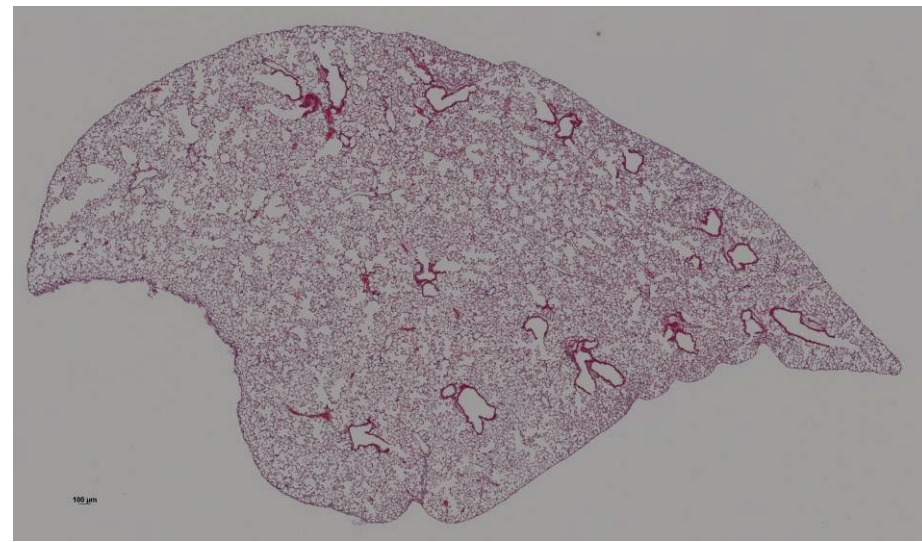
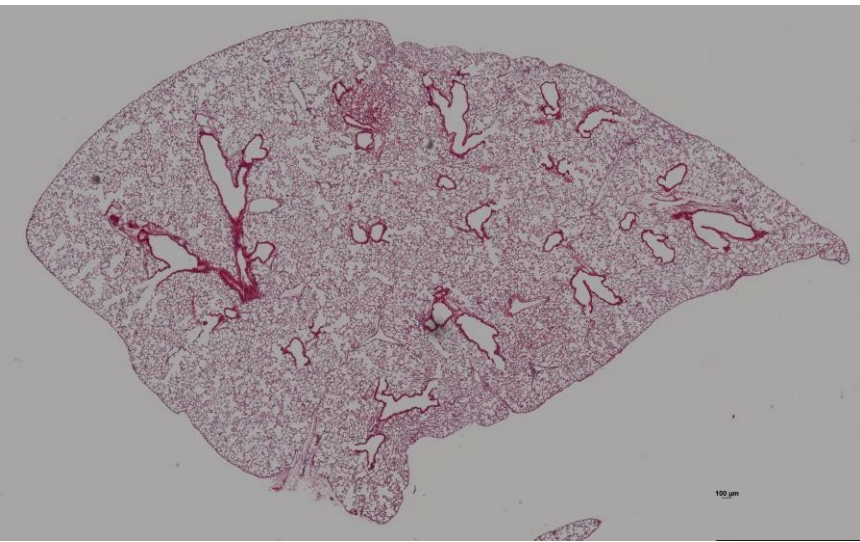
C

AAT KO 2&1 Units LPS



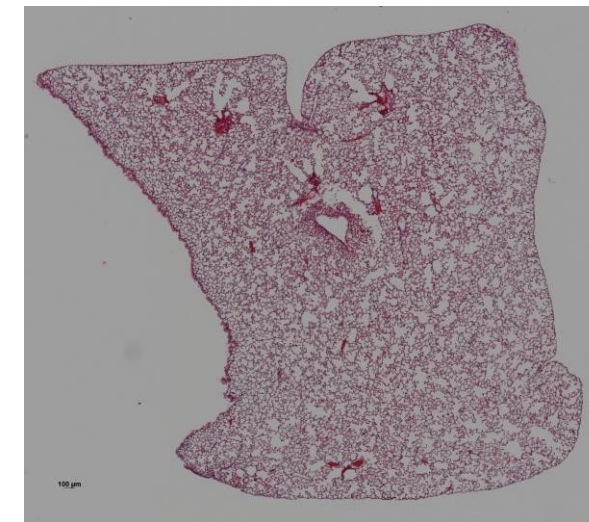
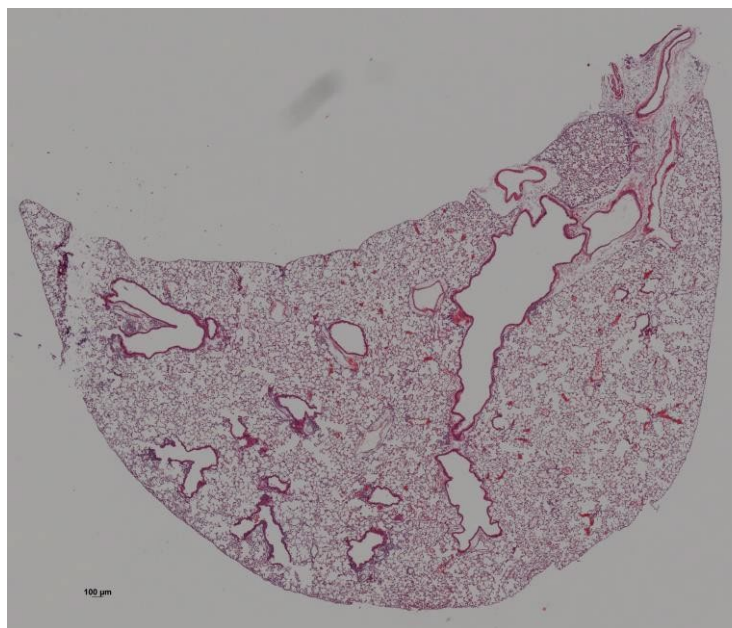
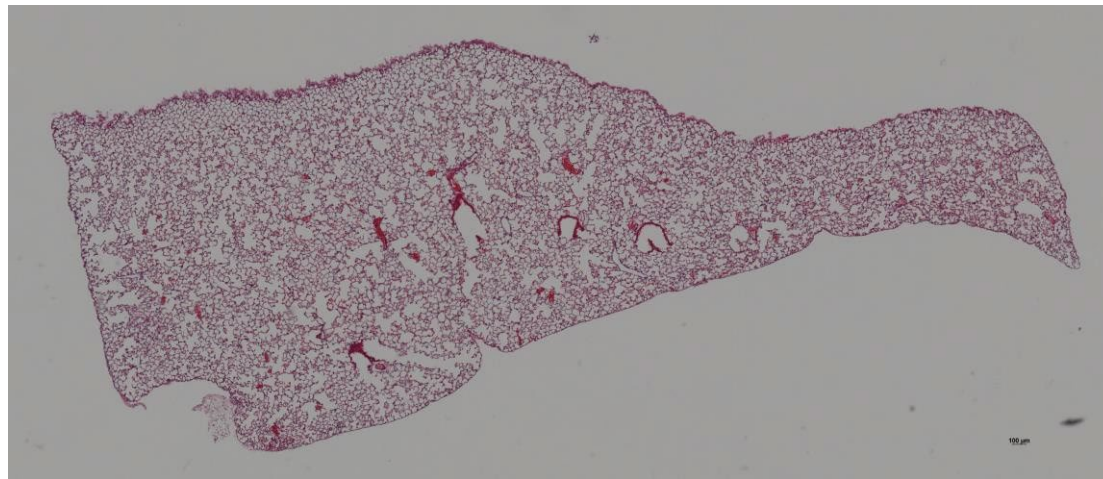
AAT KO 5&2.5 Units LPS

D



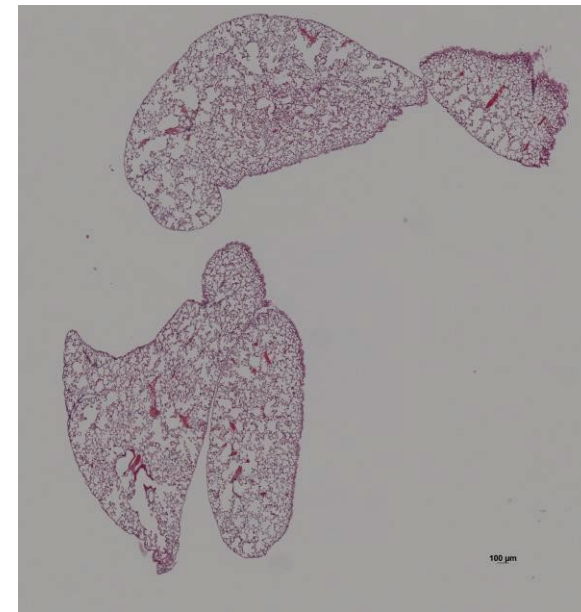
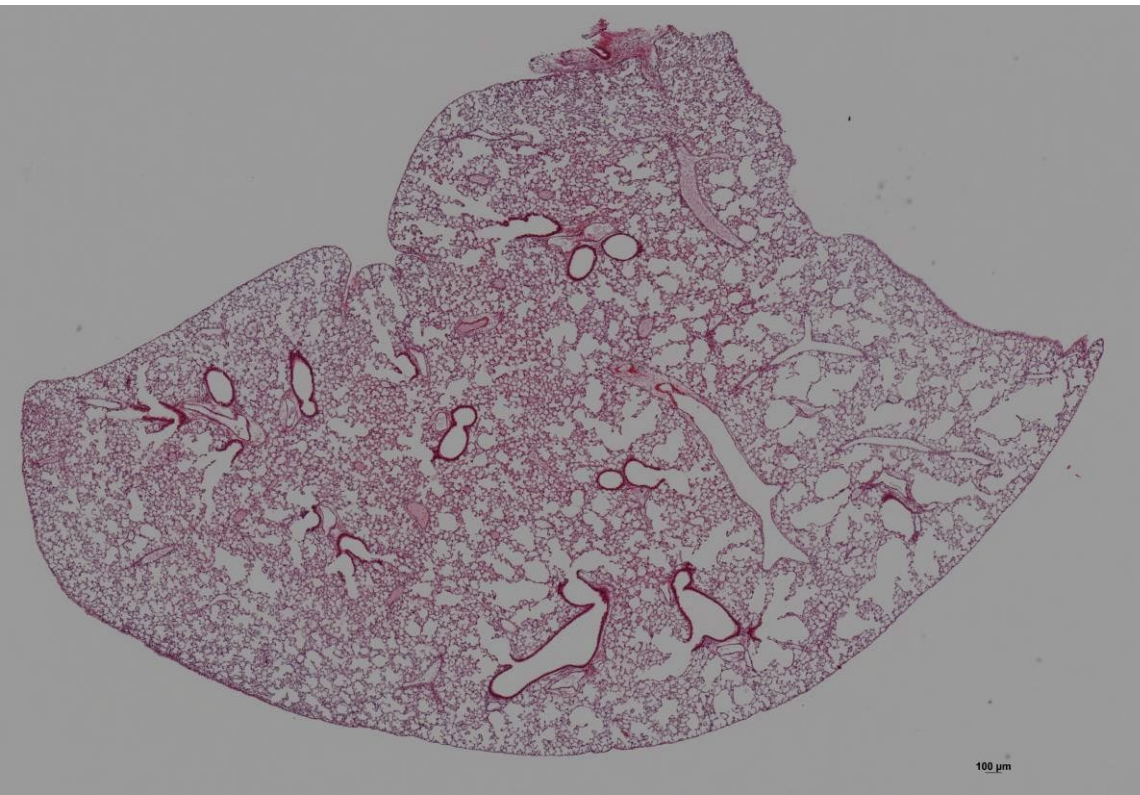
E

AAT KO 10&5 Units LPS

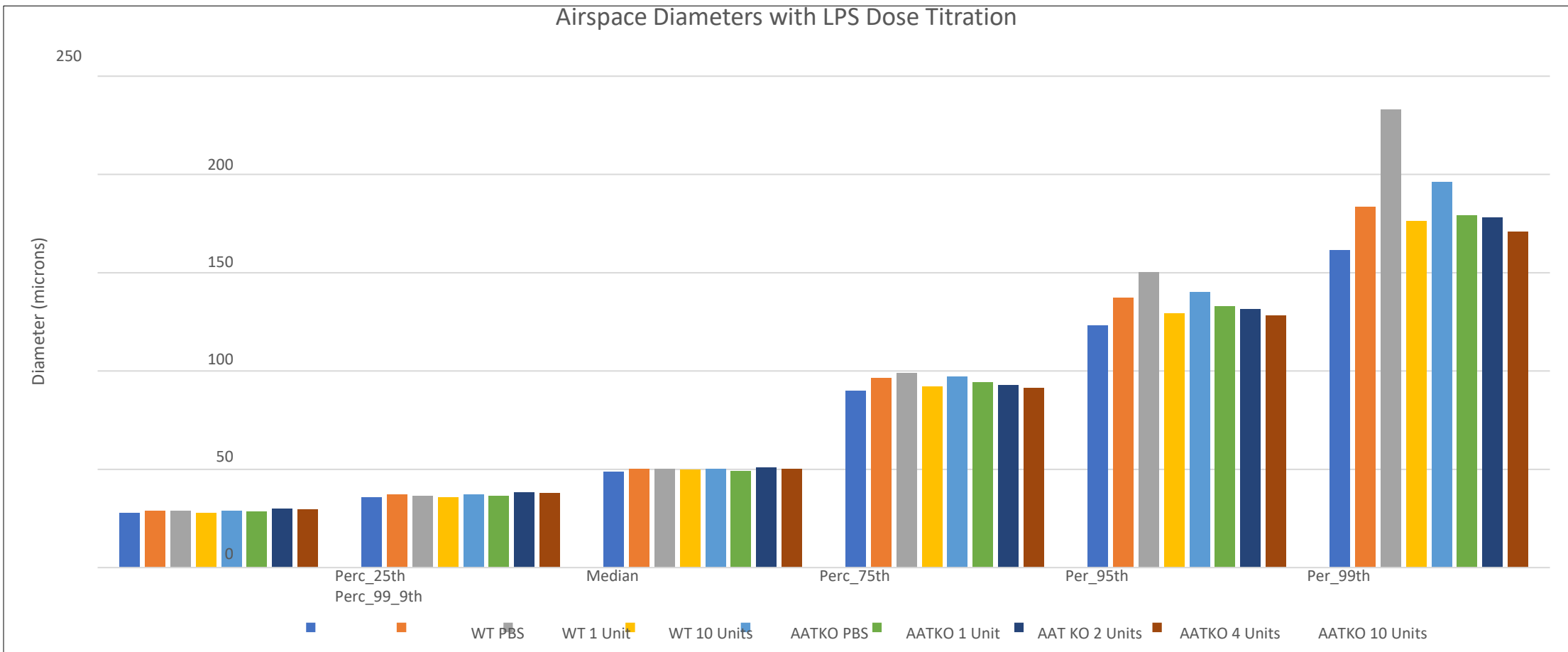


WT 10&5 Units LPS

F

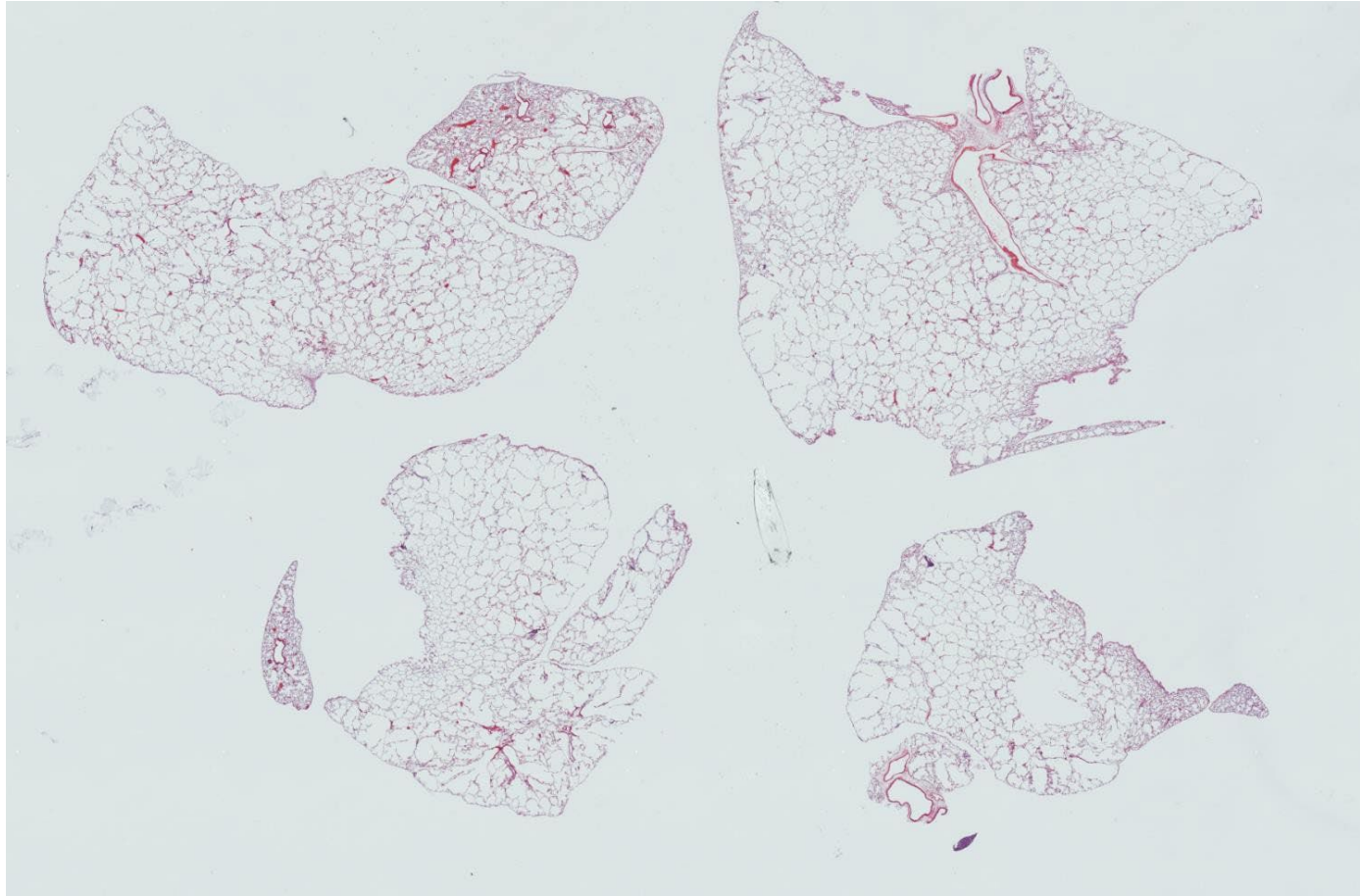


G

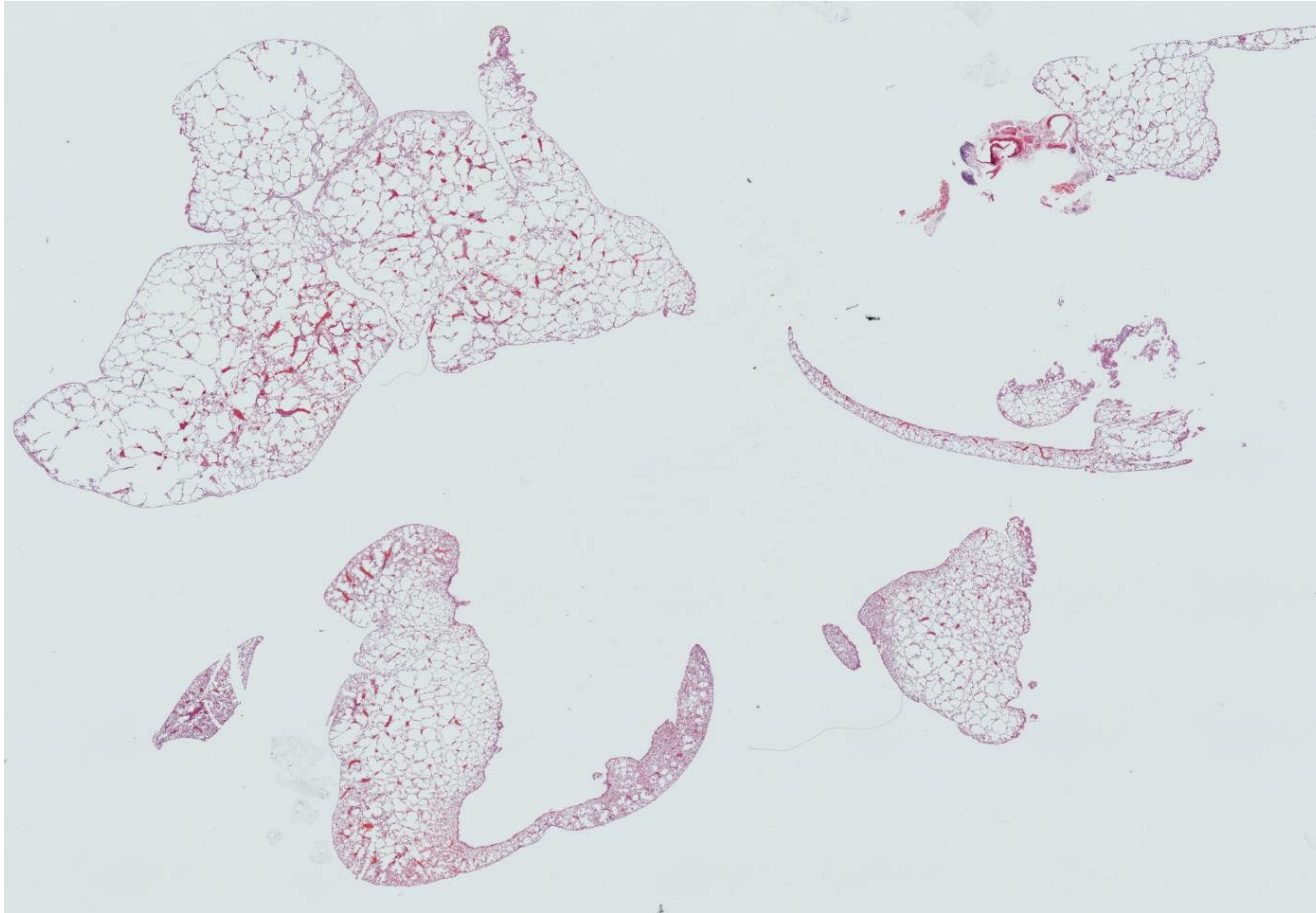


Titration of Tracheal PPE Dose in AAT-deficient Mice

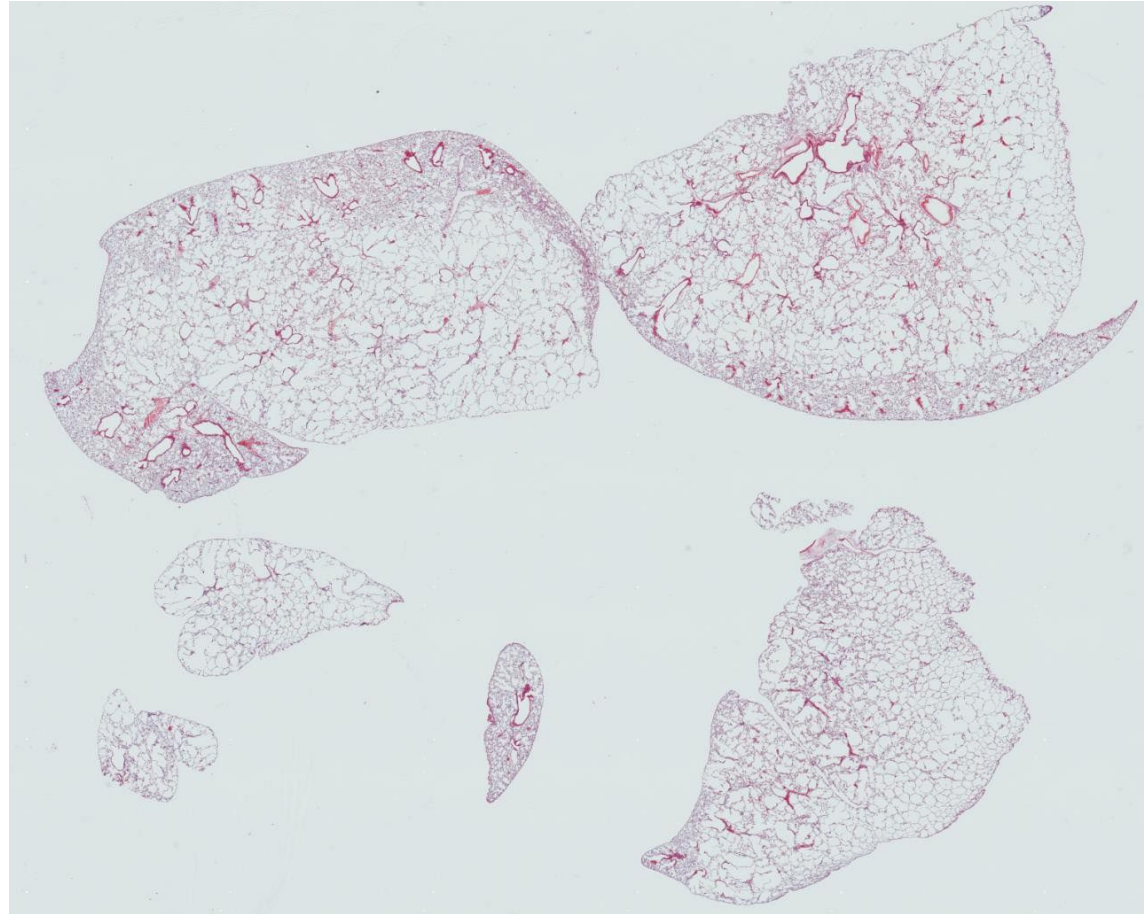
2659 AAT-KO 0.25 U



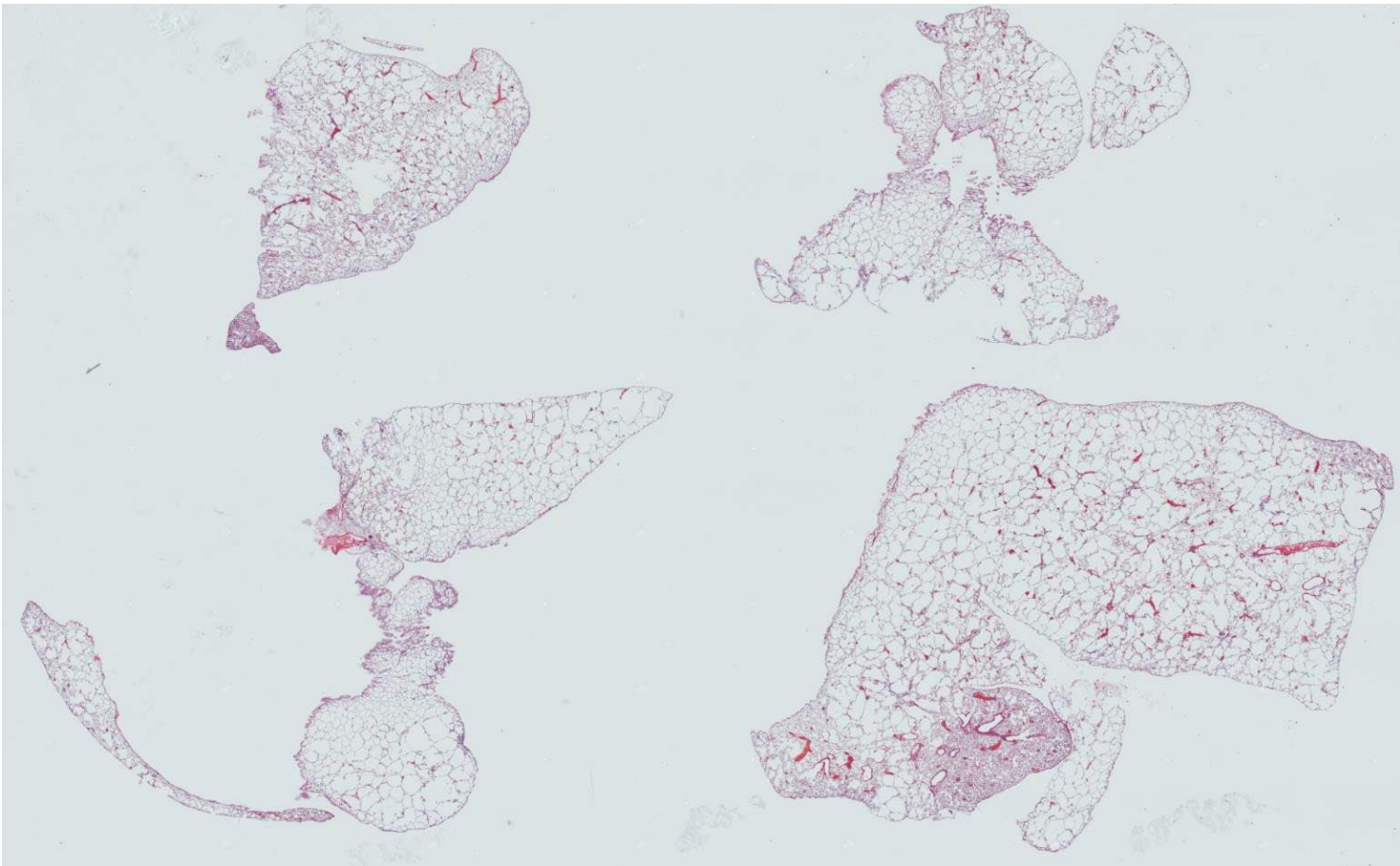
2683 AAT-KO 0.25 U



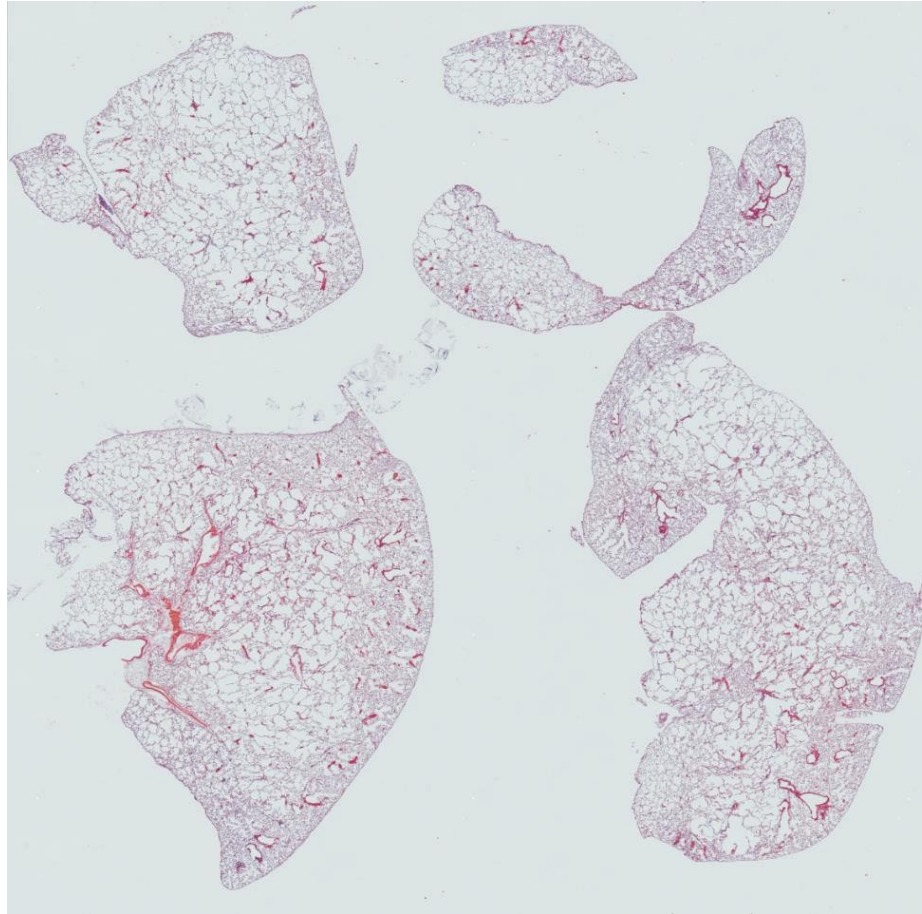
2688 AAT-KO 0.25 U



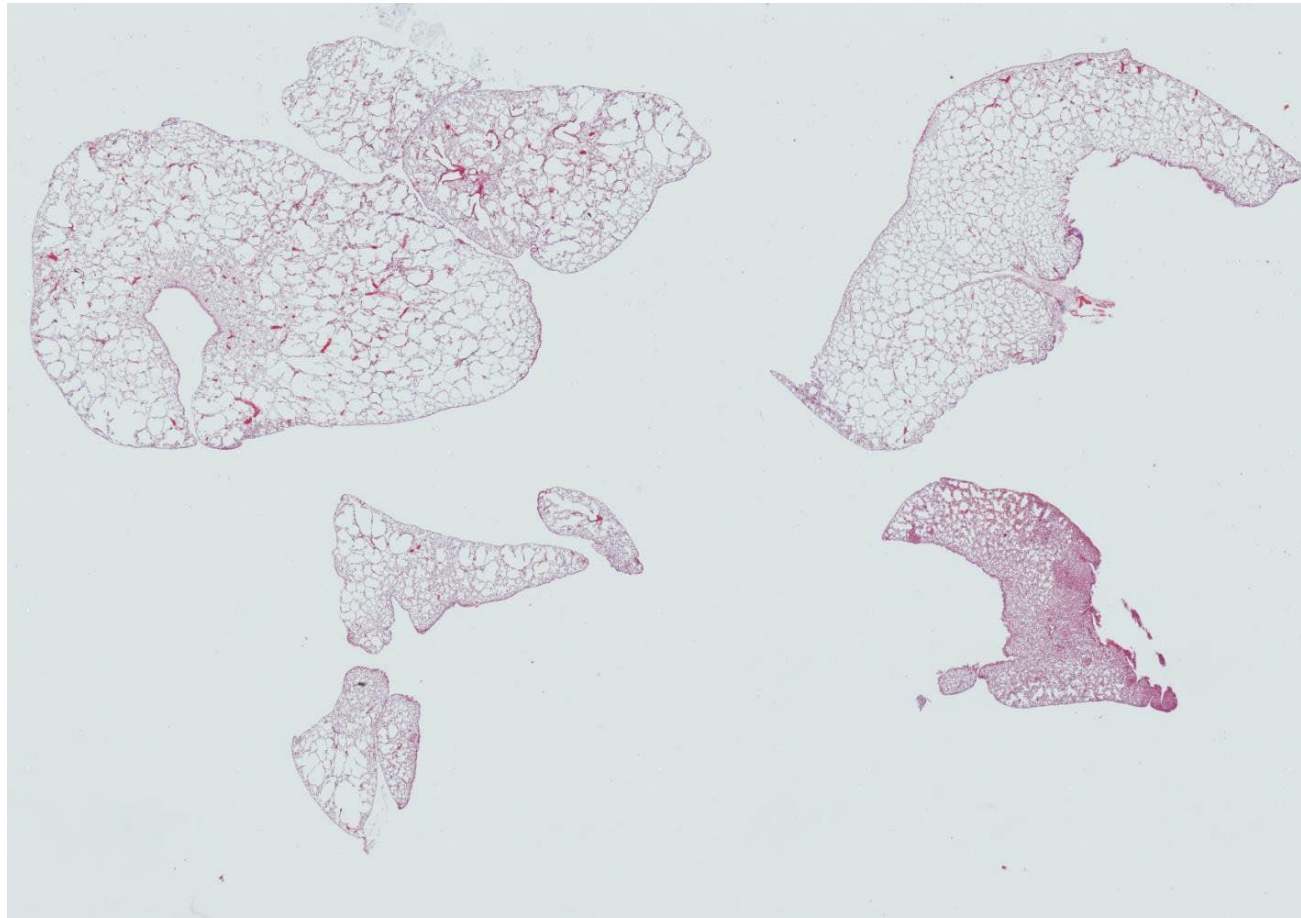
2724 AAT-KO 0.5 U



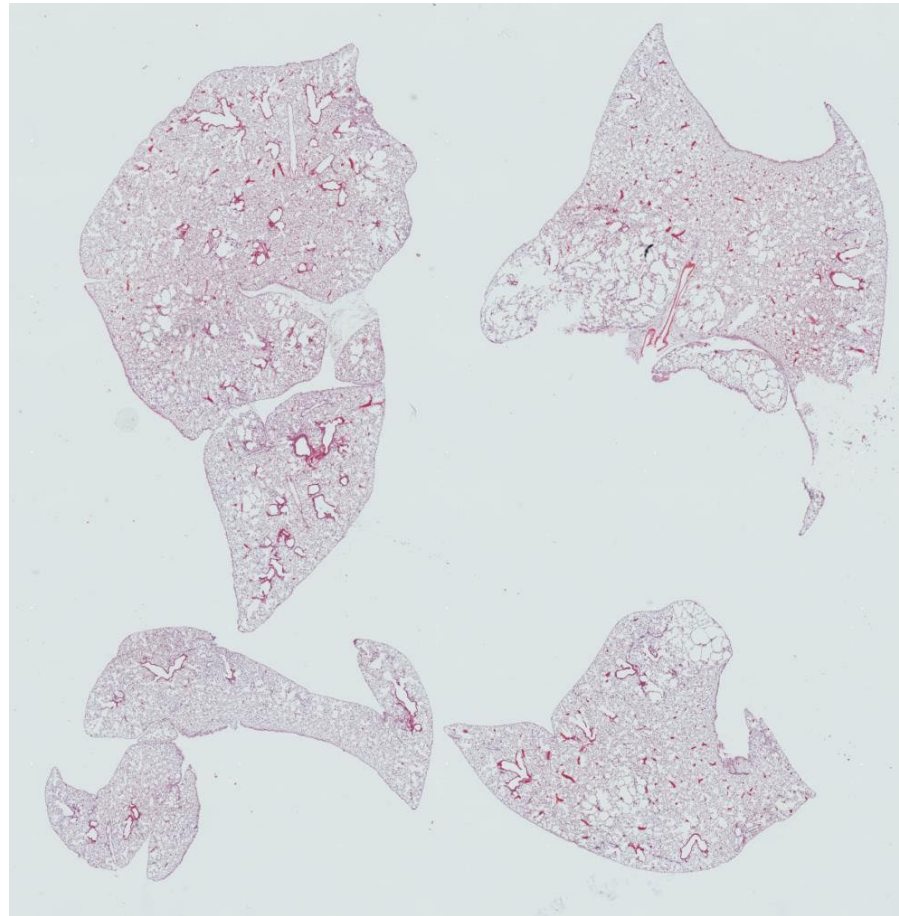
2725 AAT-KO 0.5 U



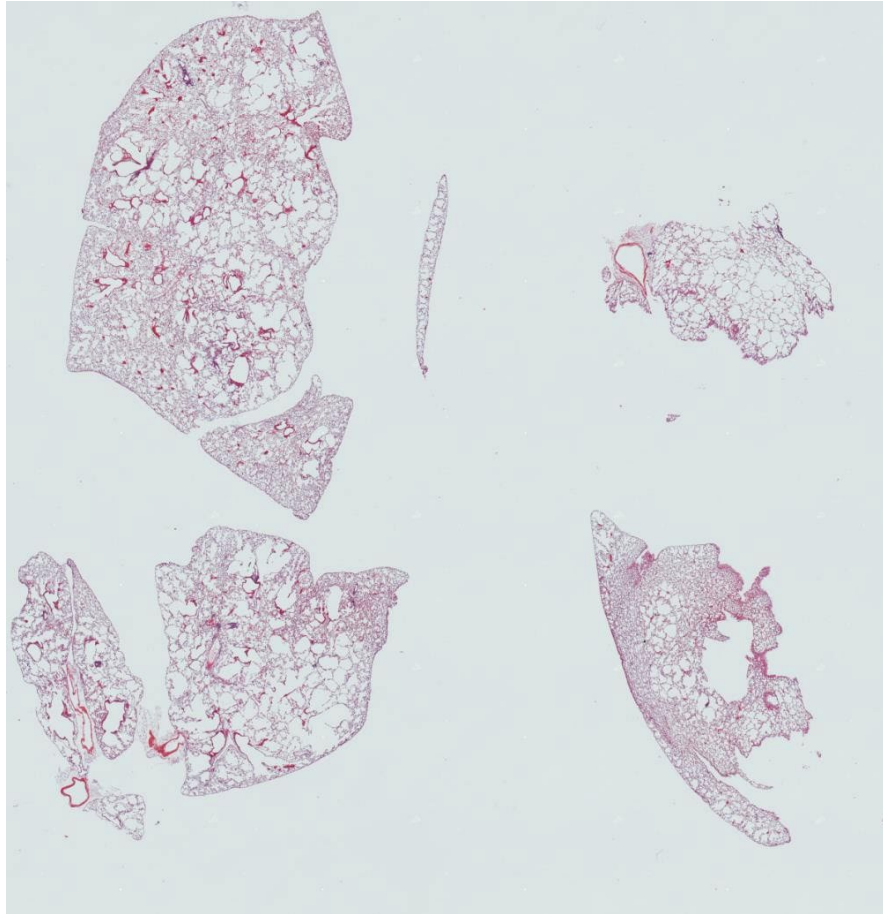
2726 AAT-KO 0.5 U



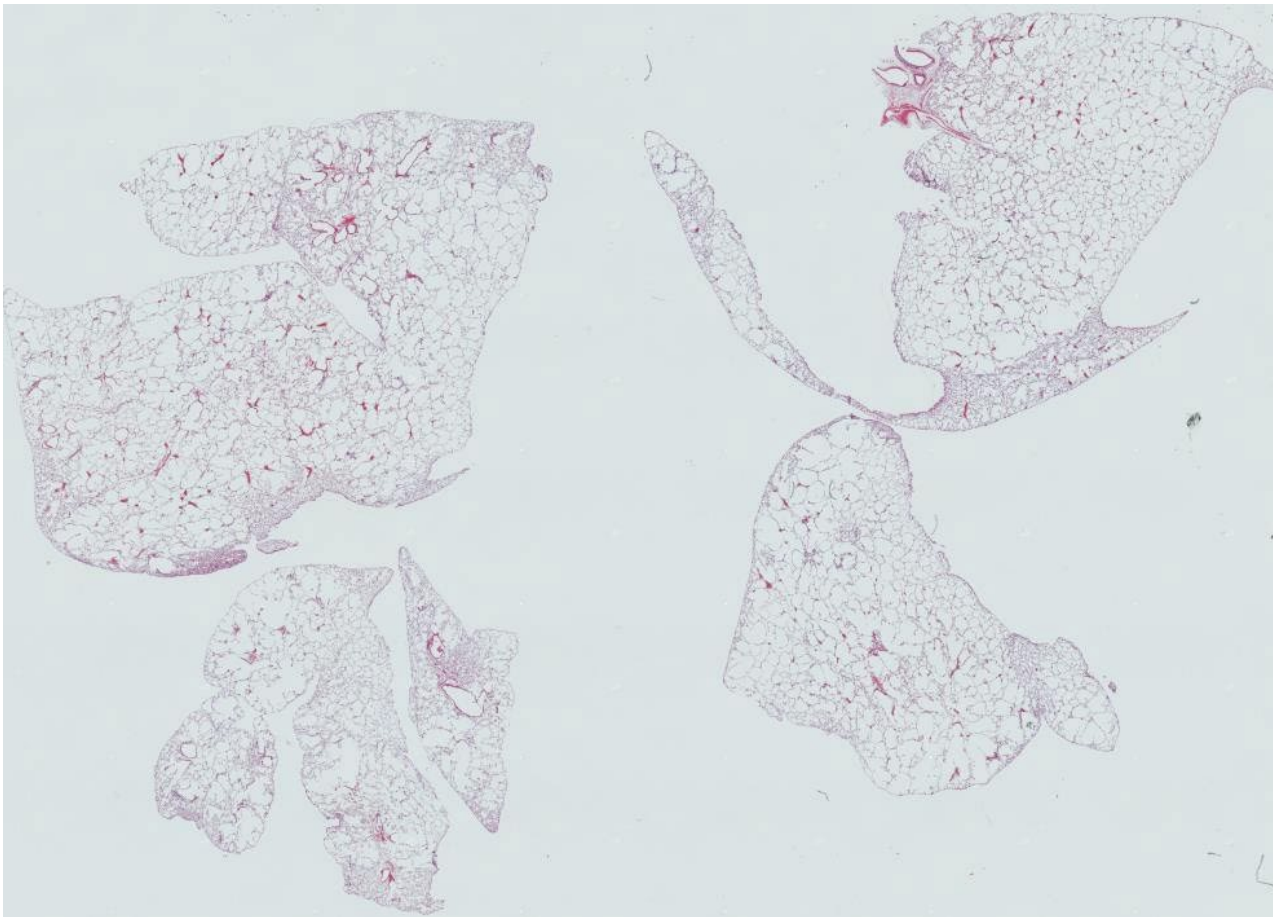
2677 AAT-KO 0.5 U



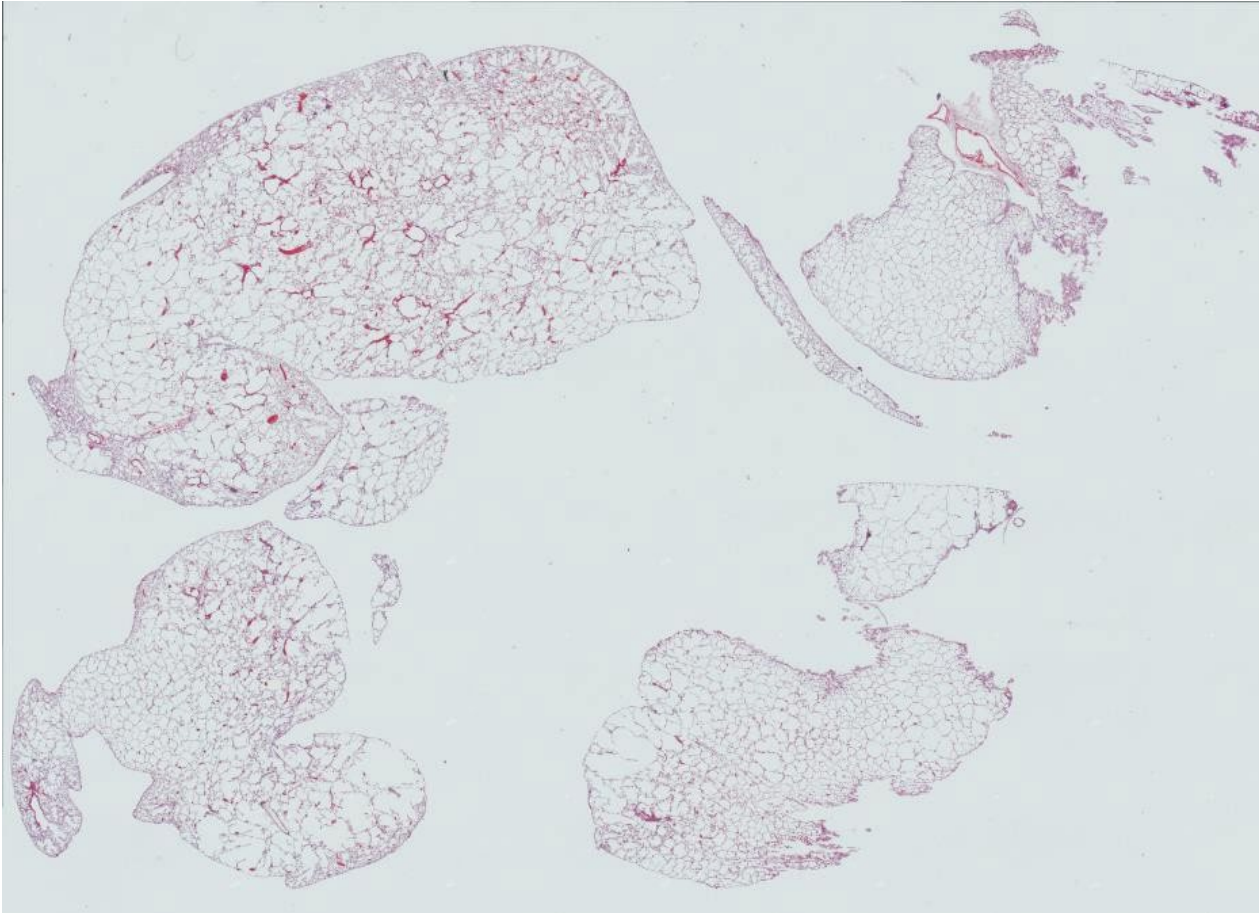
2680 AAT-KO 0.5 U



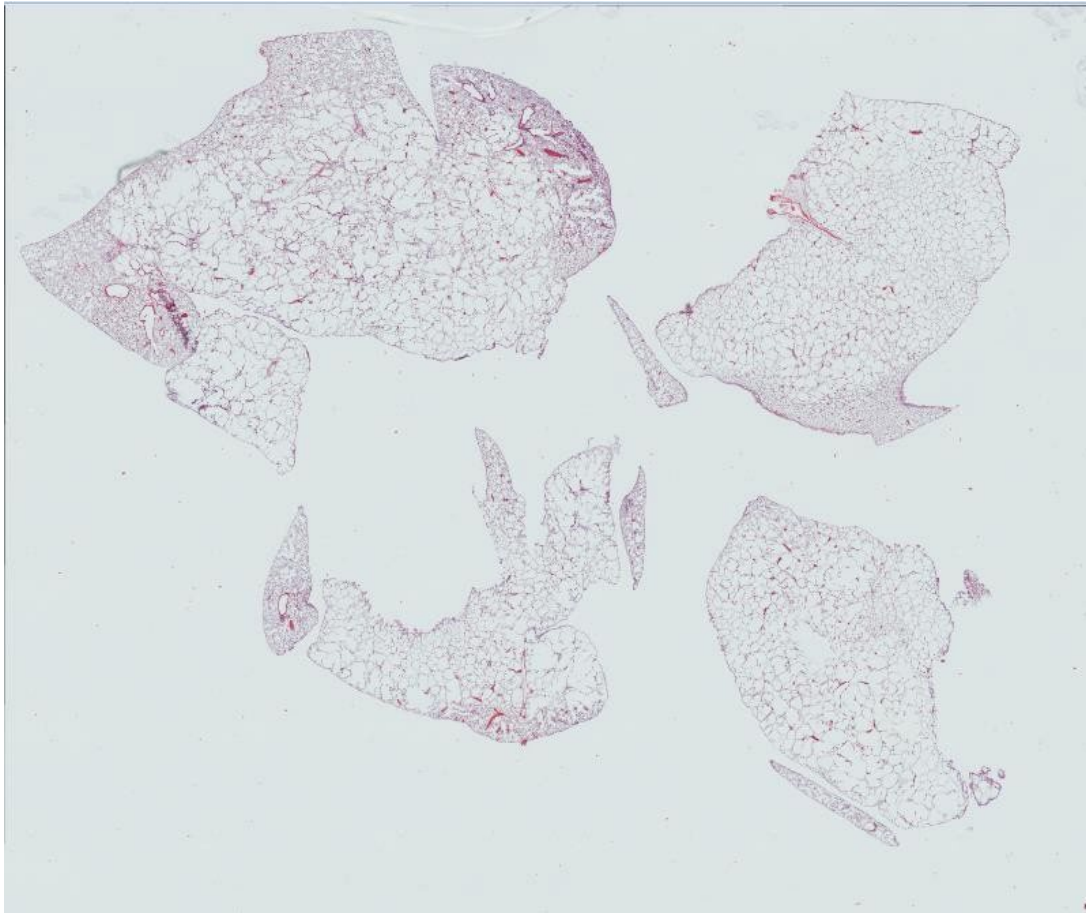
2685 AAT-KO 1.0 U



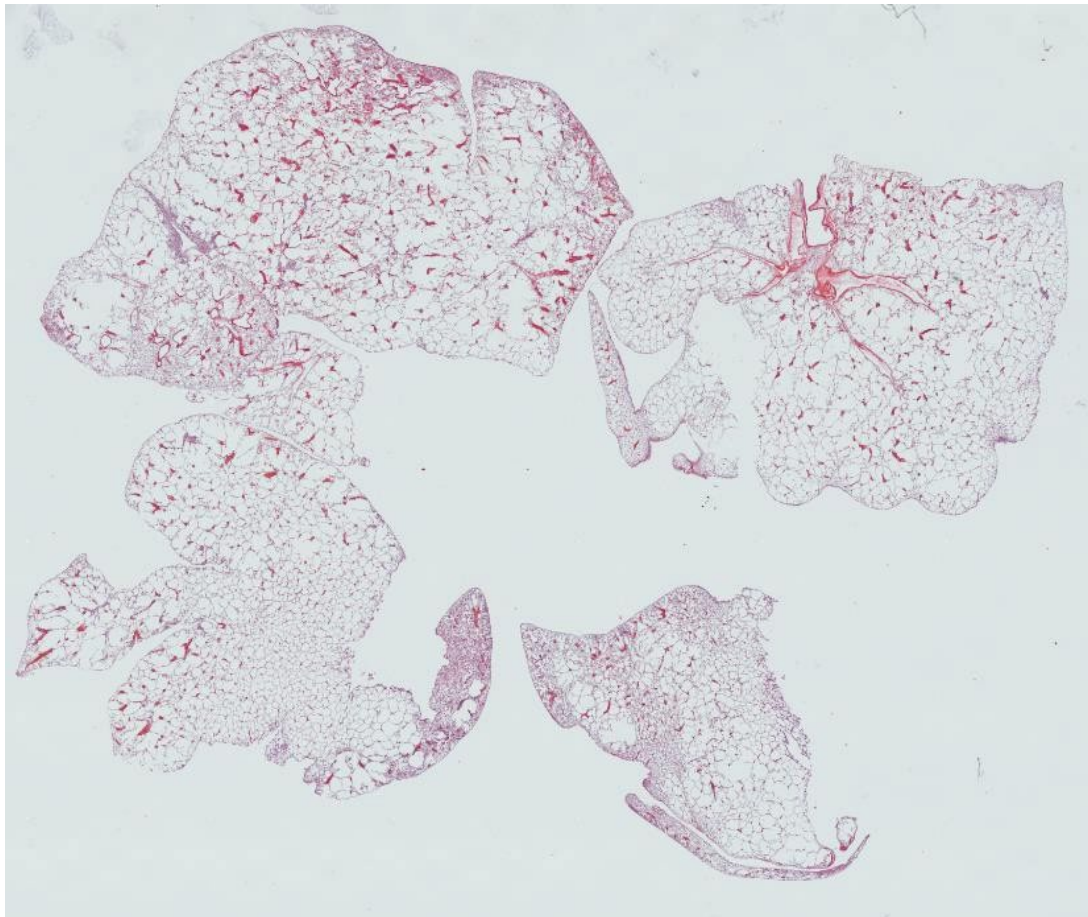
2729 AAT-KO 1.0 U



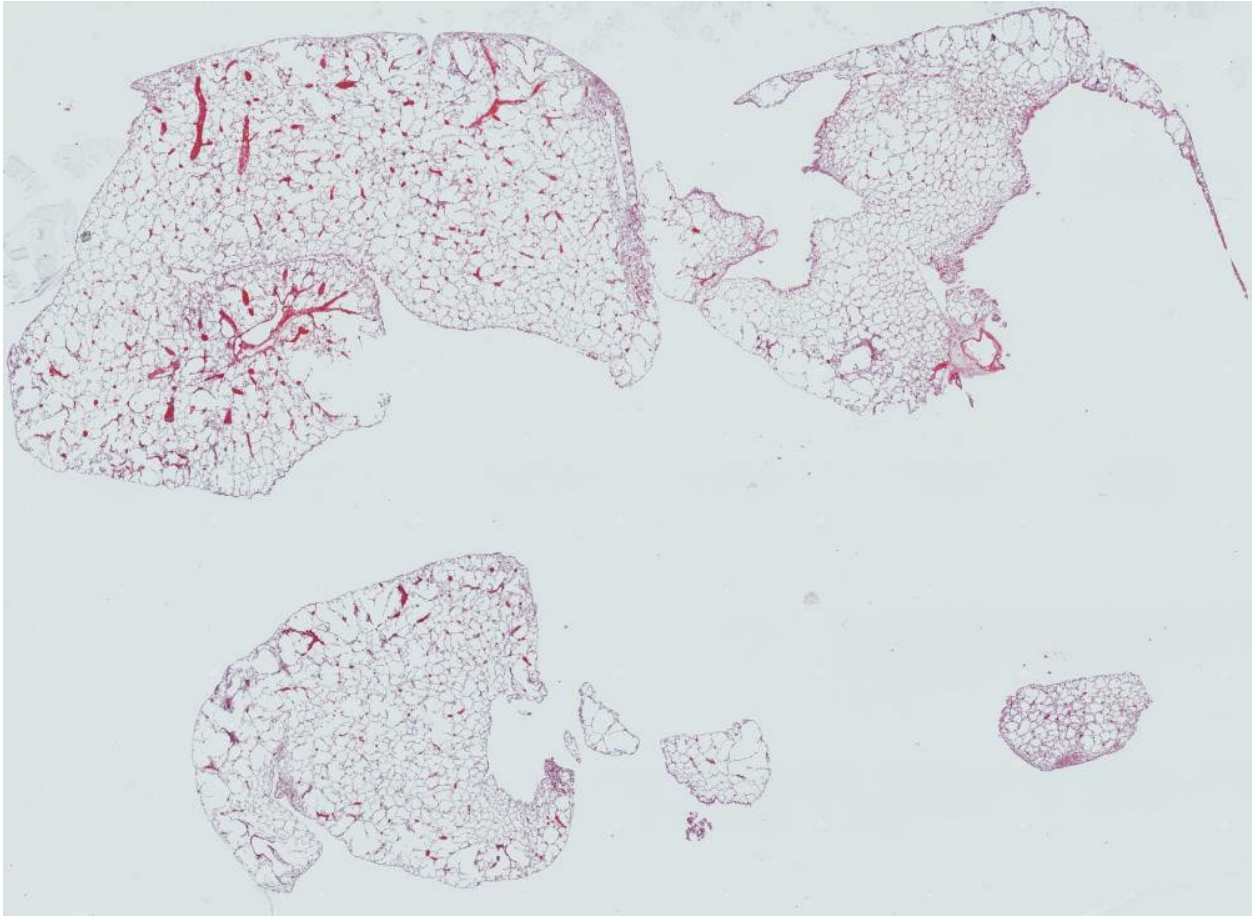
2686 AAT-KO 1.0 U



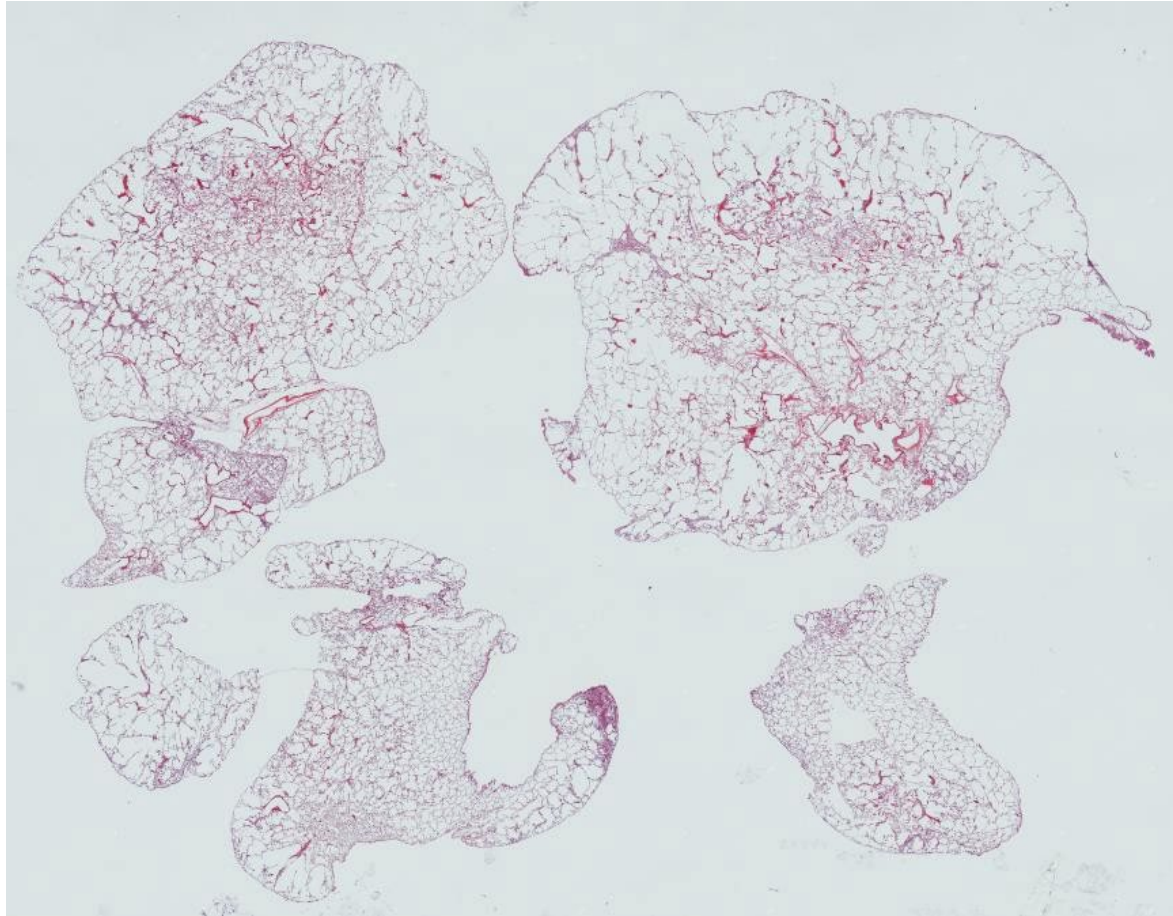
2687 AAT-KO 1.0 U



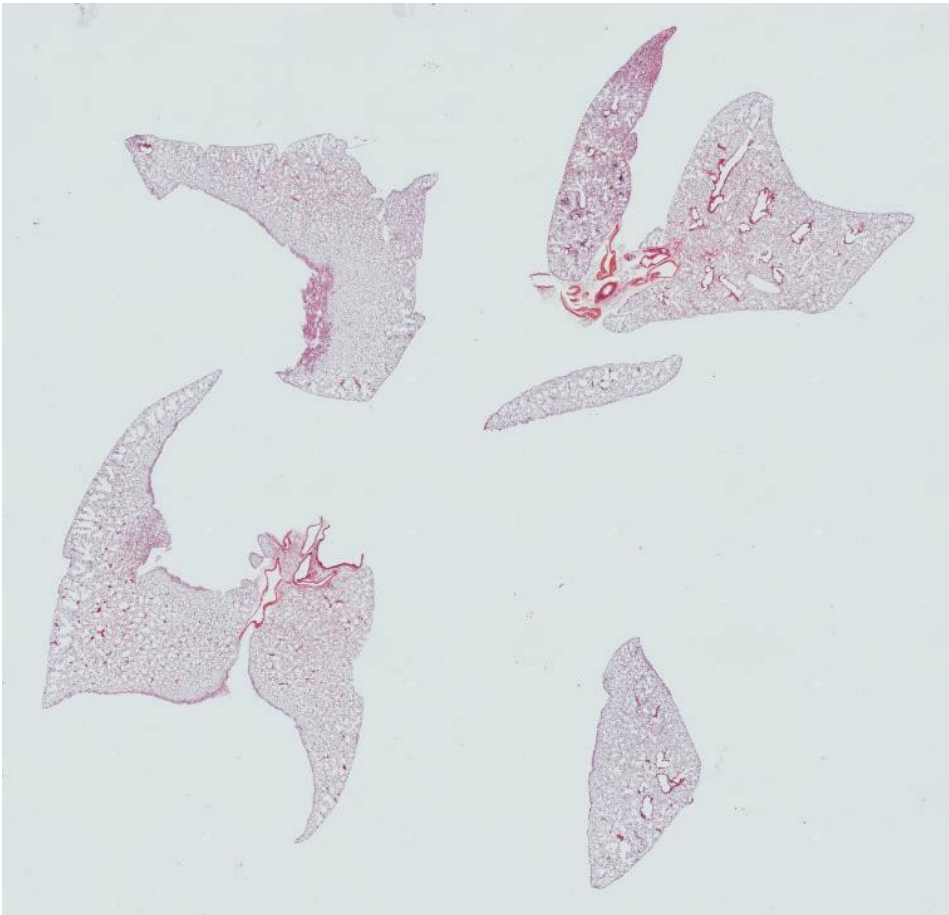
2681 AAT-KO 2.0 U



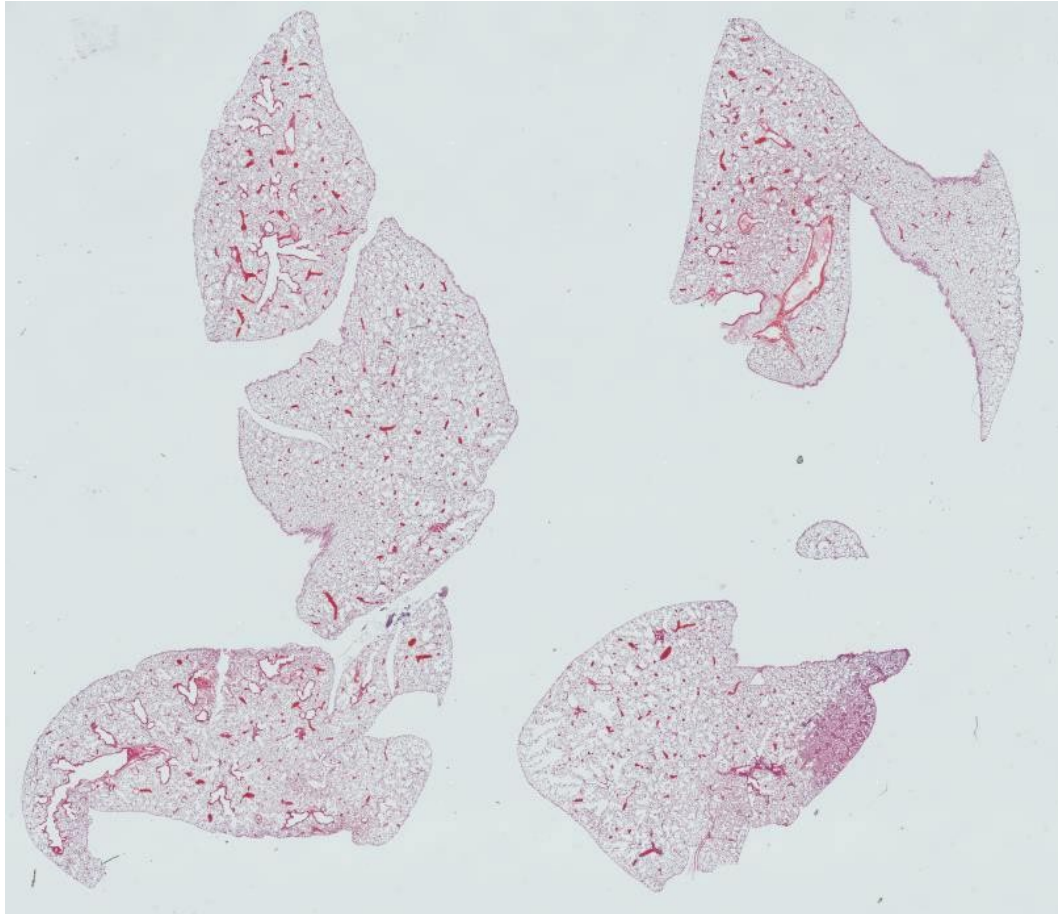
2682 AAT-KO 2.0 U



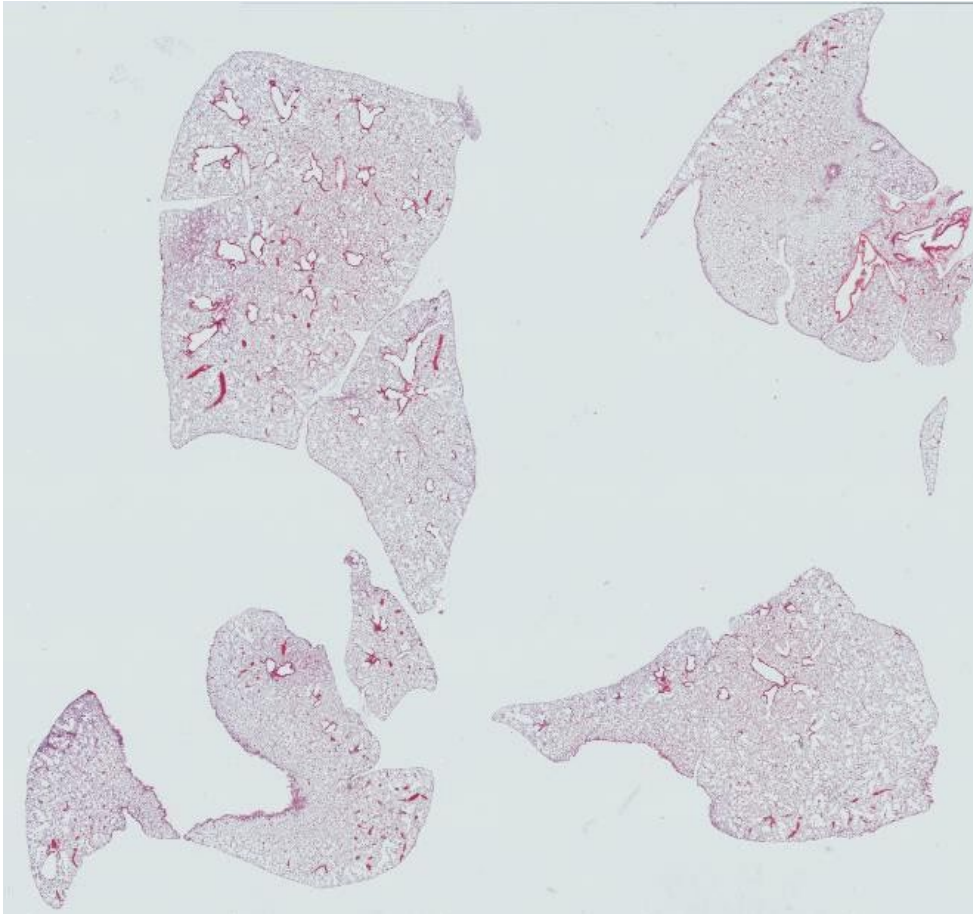
2678 AAT-KO PBS



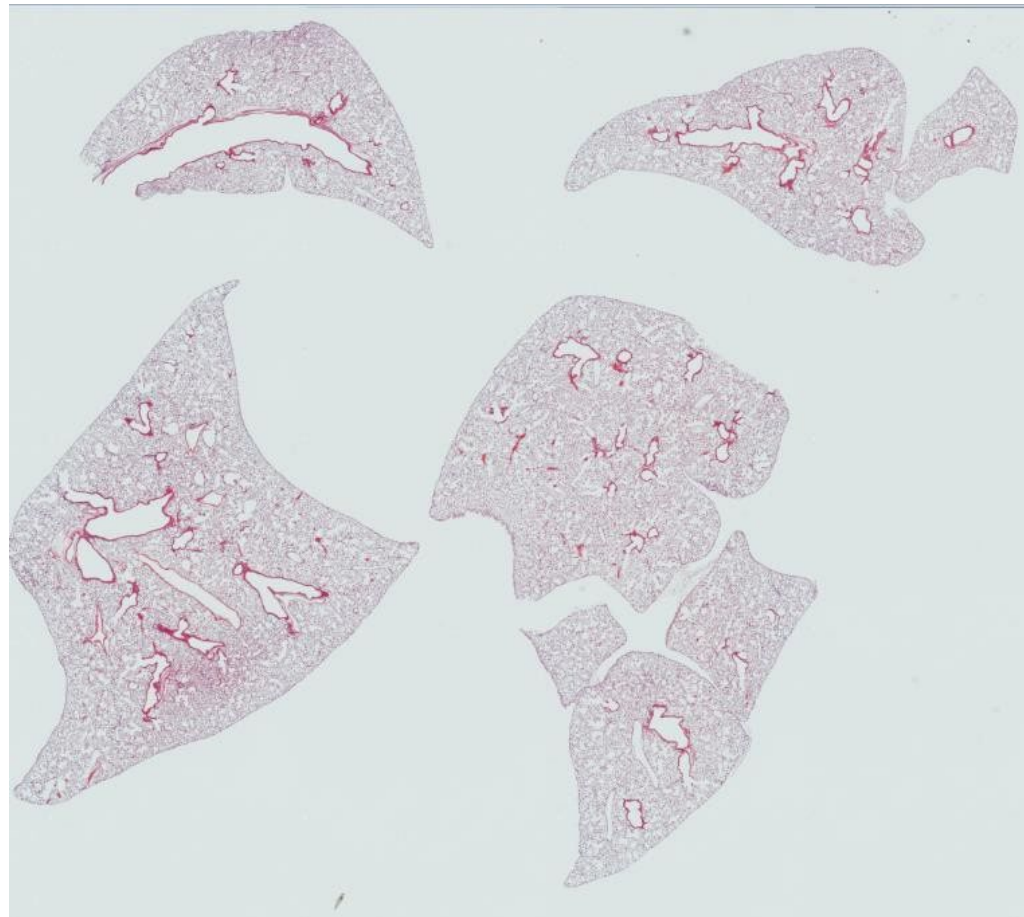
2723 AAT-KO PBS



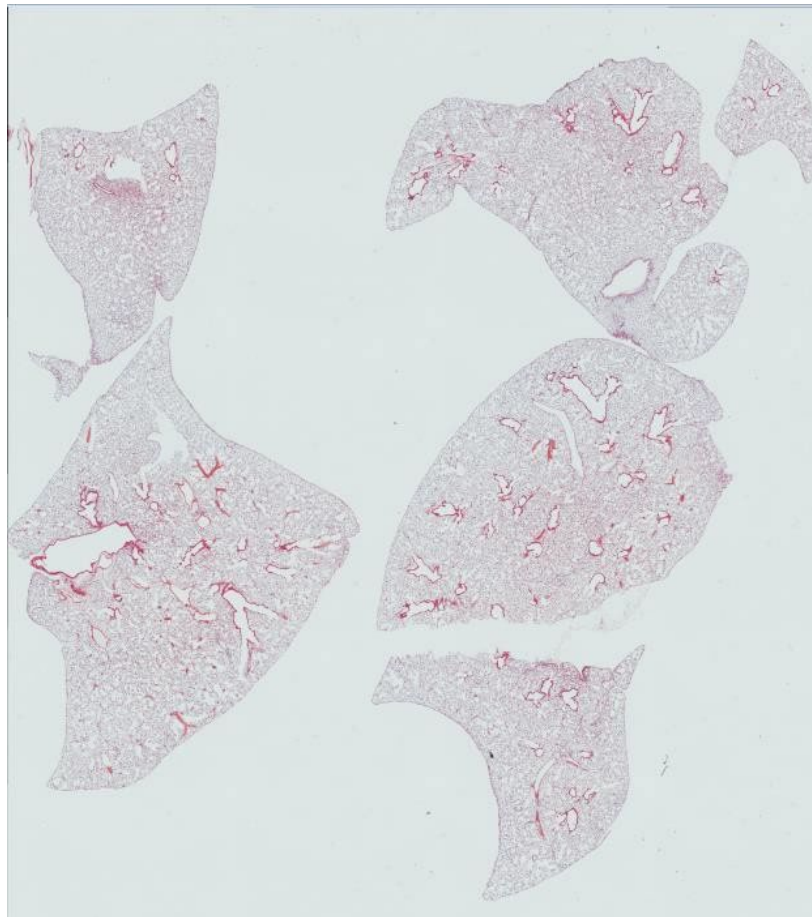
2727 AAT-KO PBS



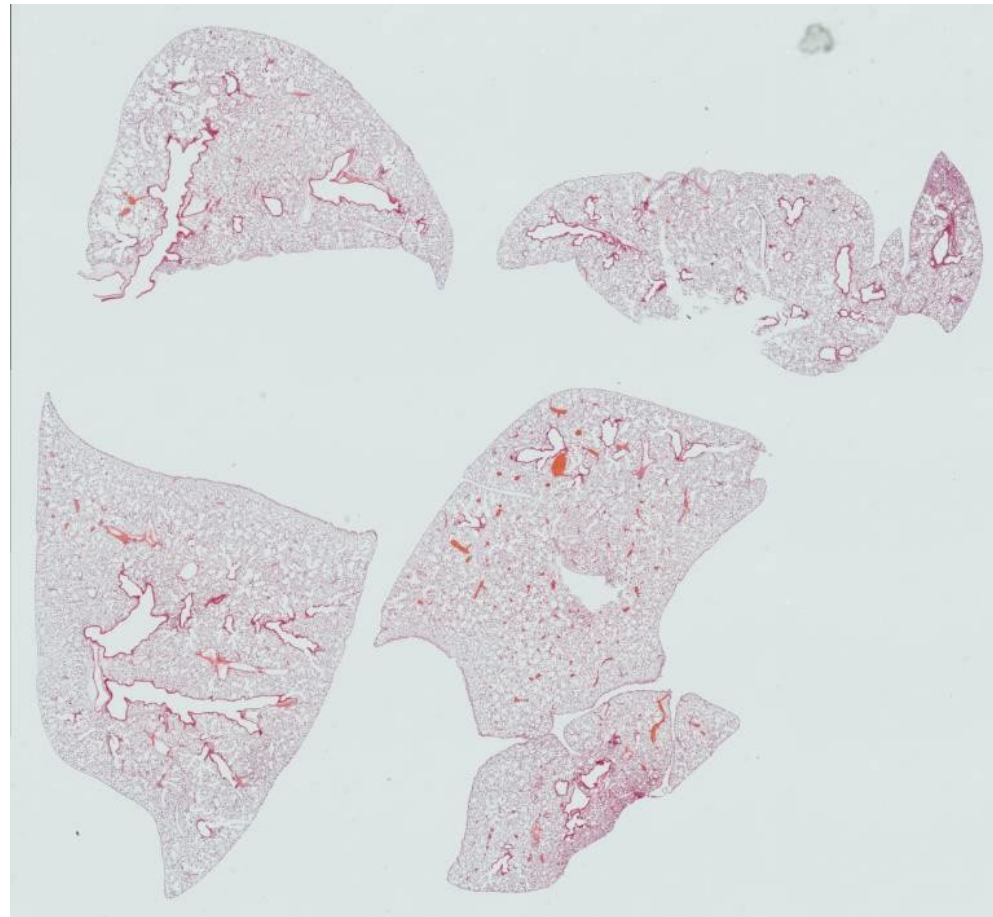
2453 WT 0.25 U



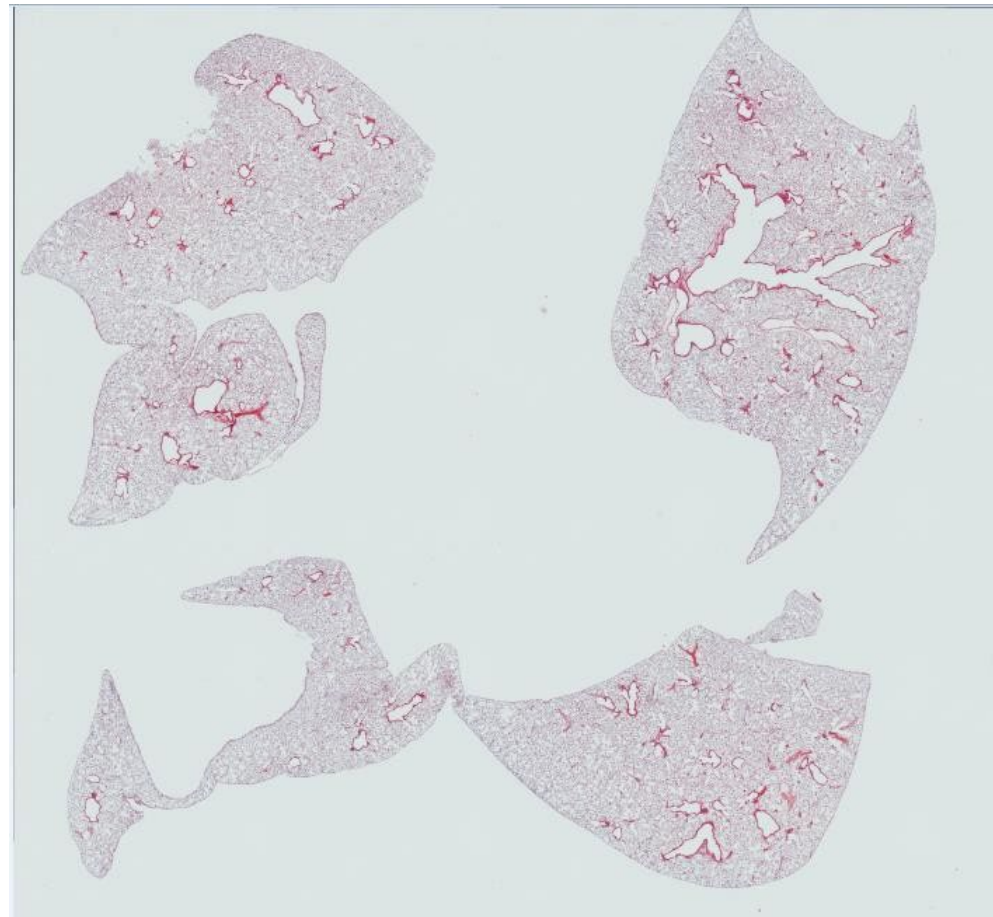
2452 WT 0.25 U



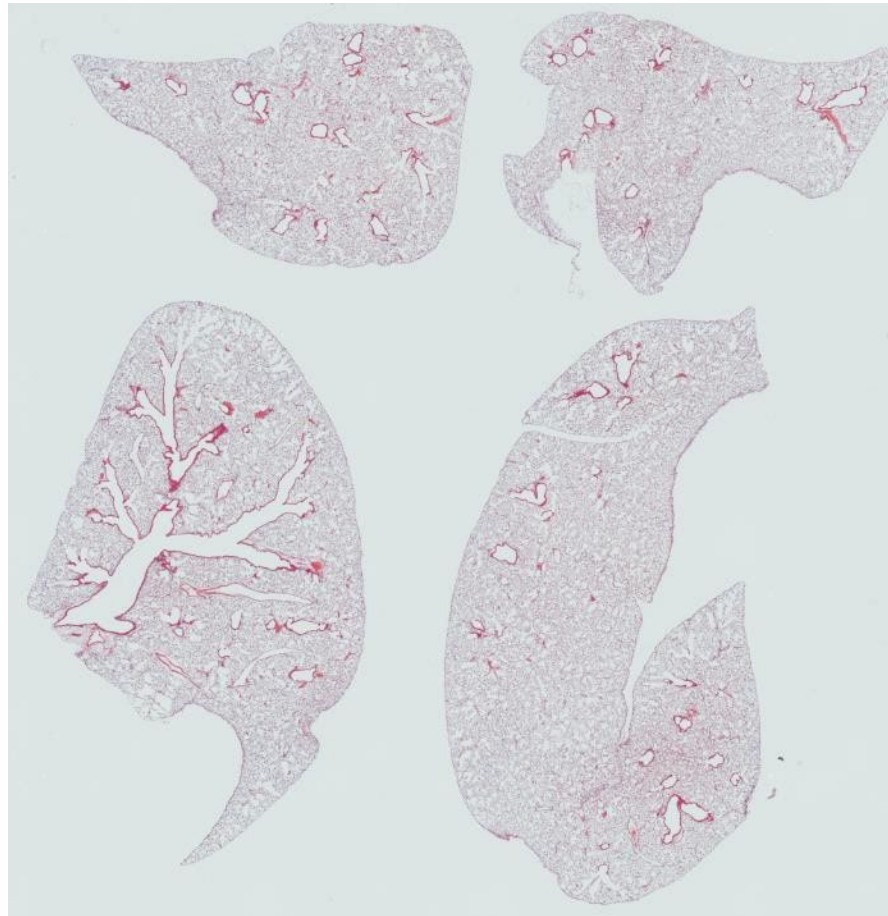
2559 WT 0.25 U



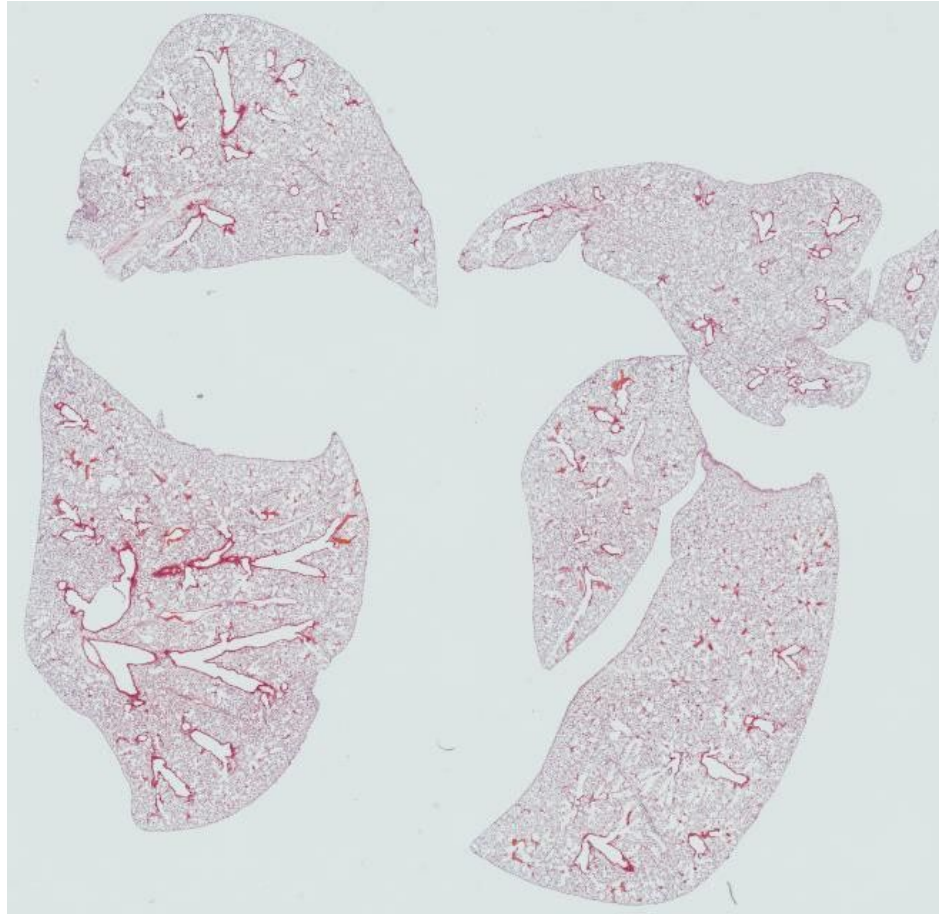
2451 WT 0.5 U



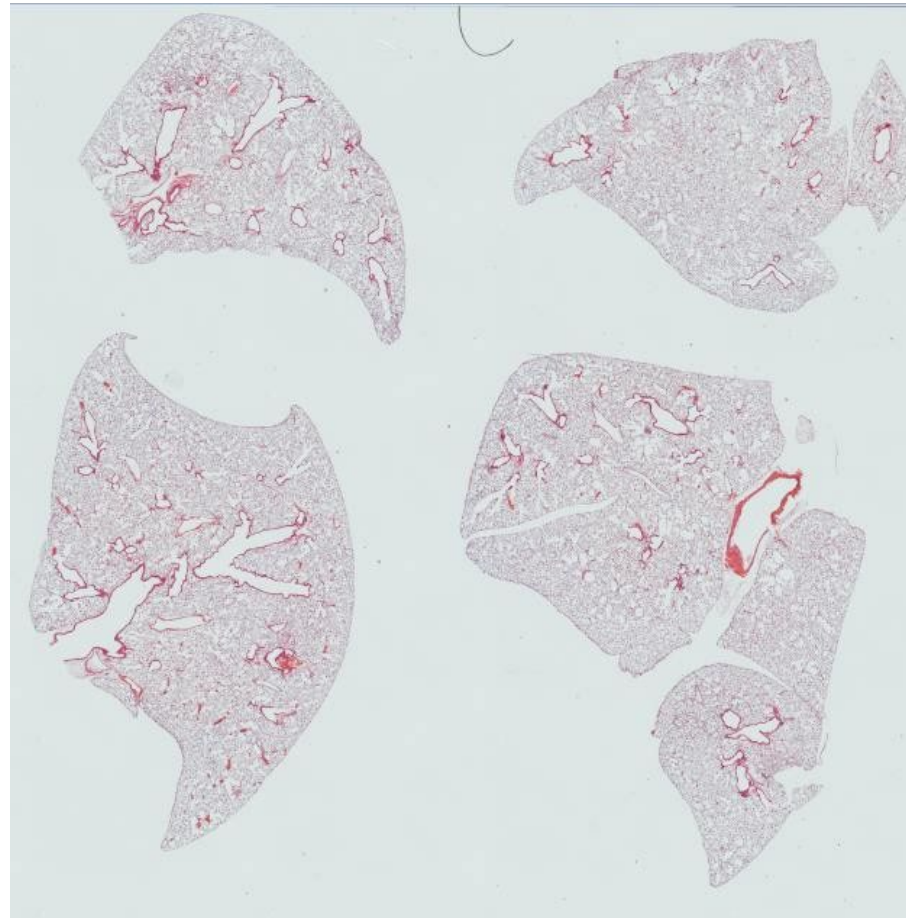
2448 WT 0.5 U



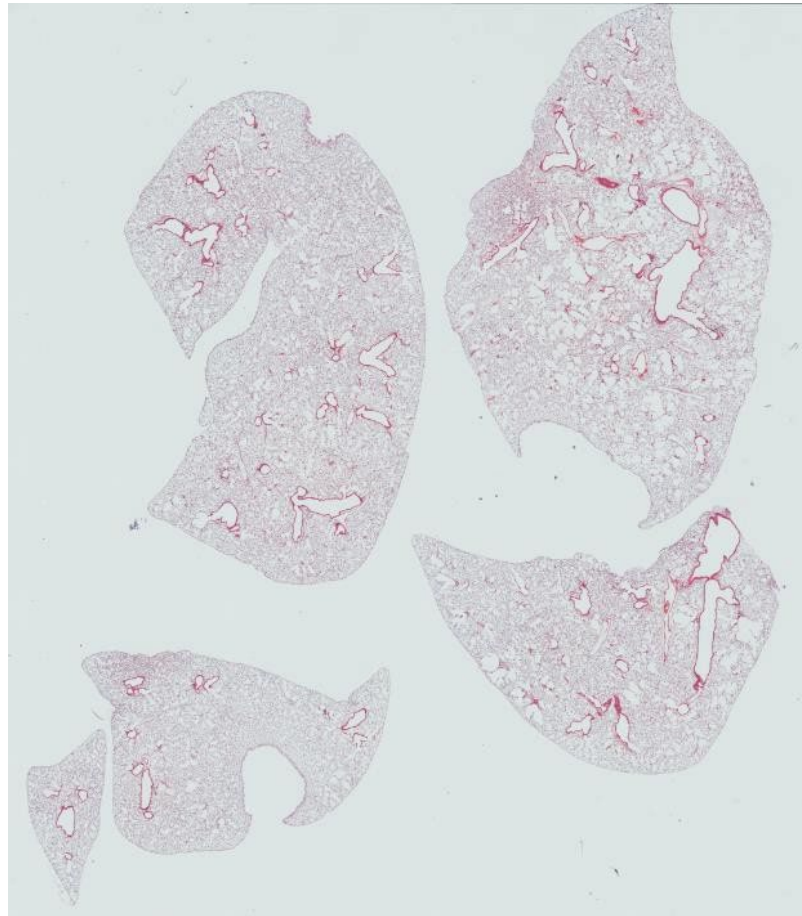
2558 WT 0.5 U



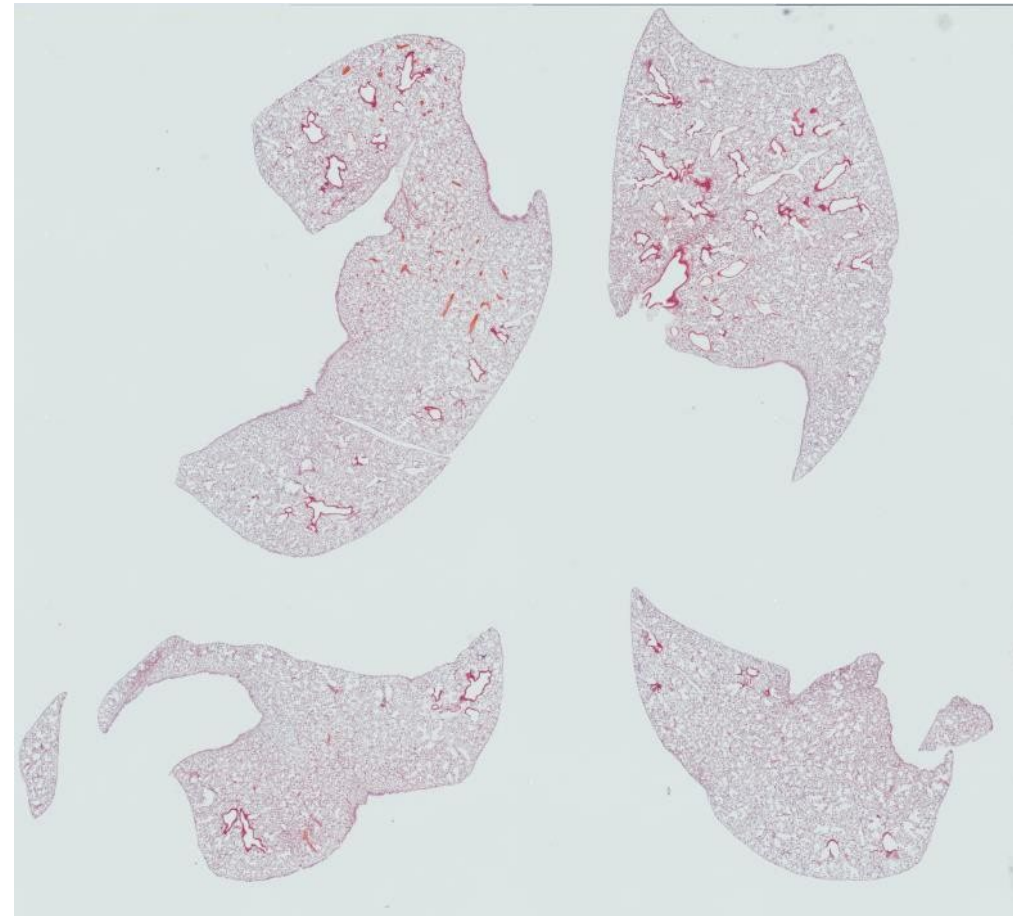
2555 WT 1.0U



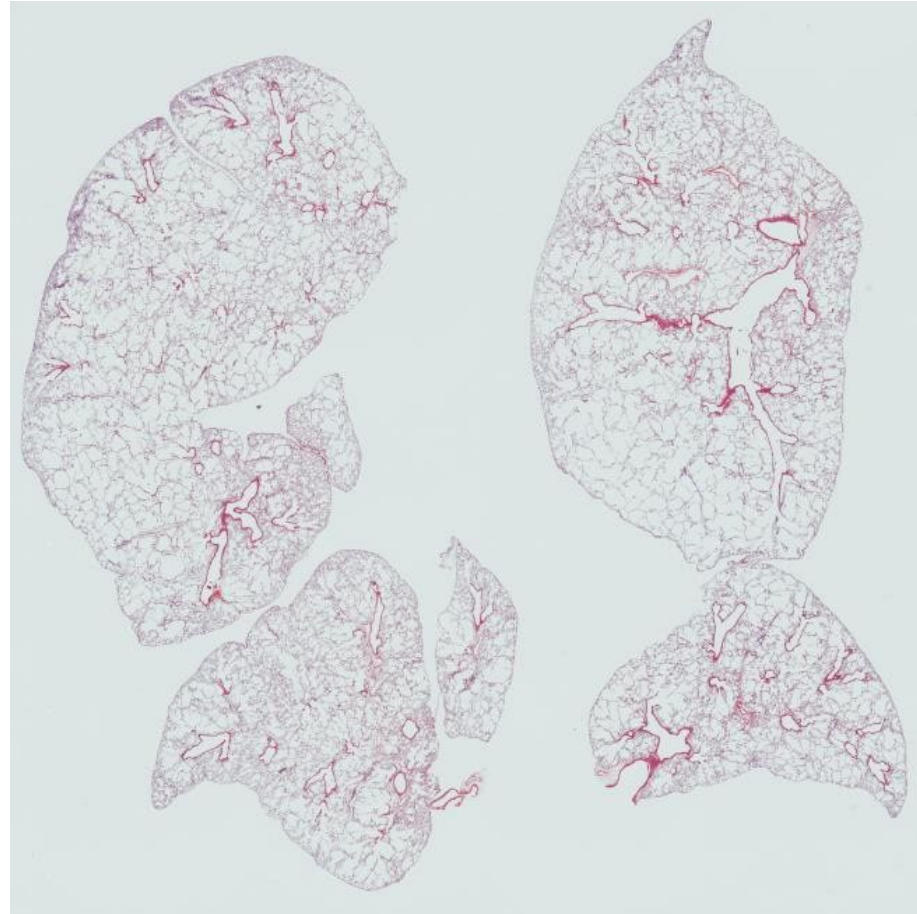
2556 WT 1.0U



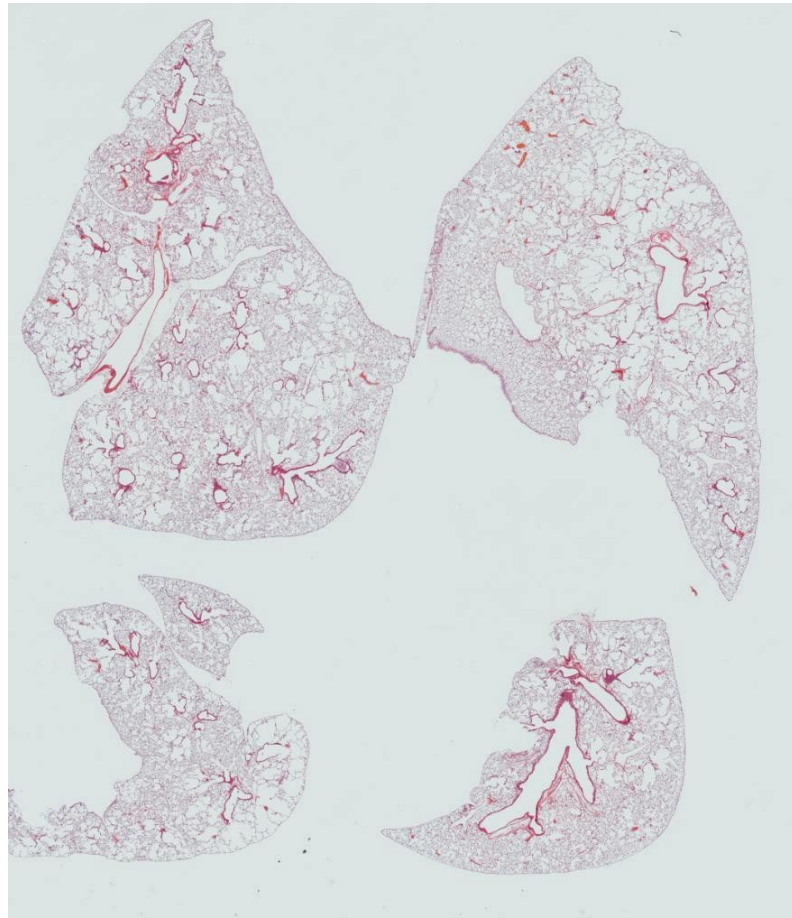
2557 WT 1.0U



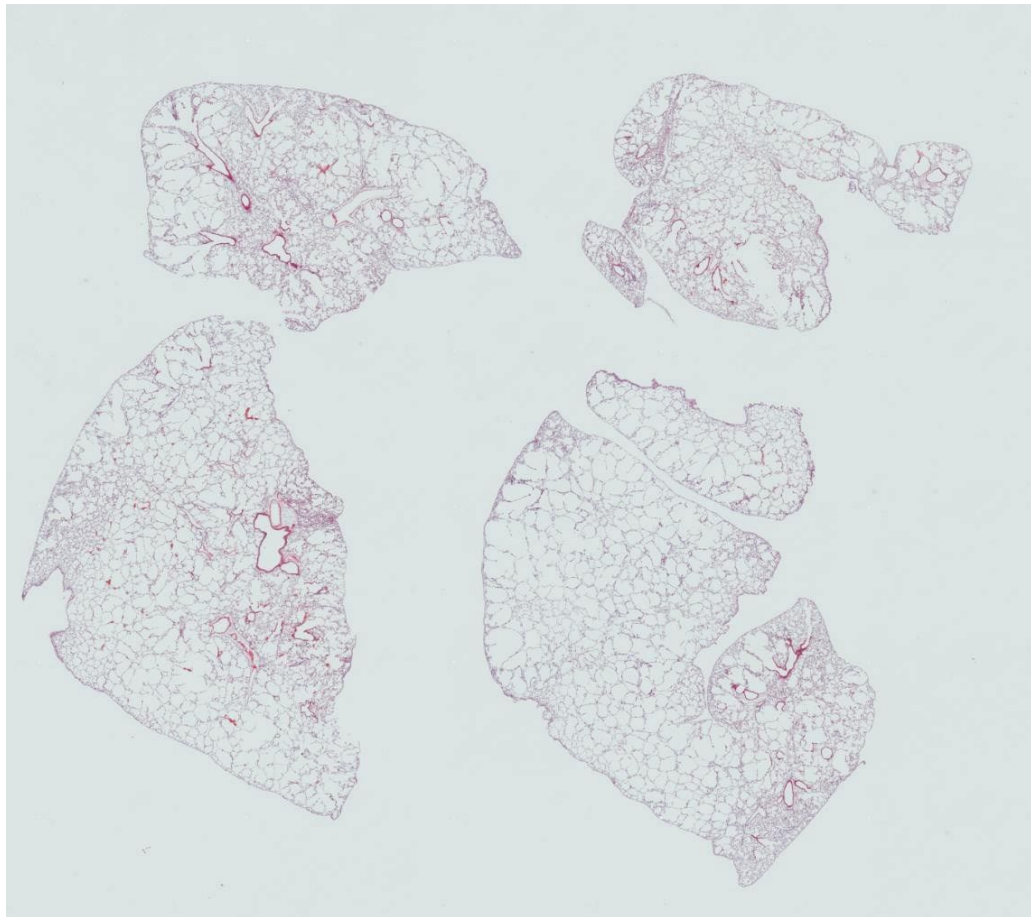
2458 WT 2.0U



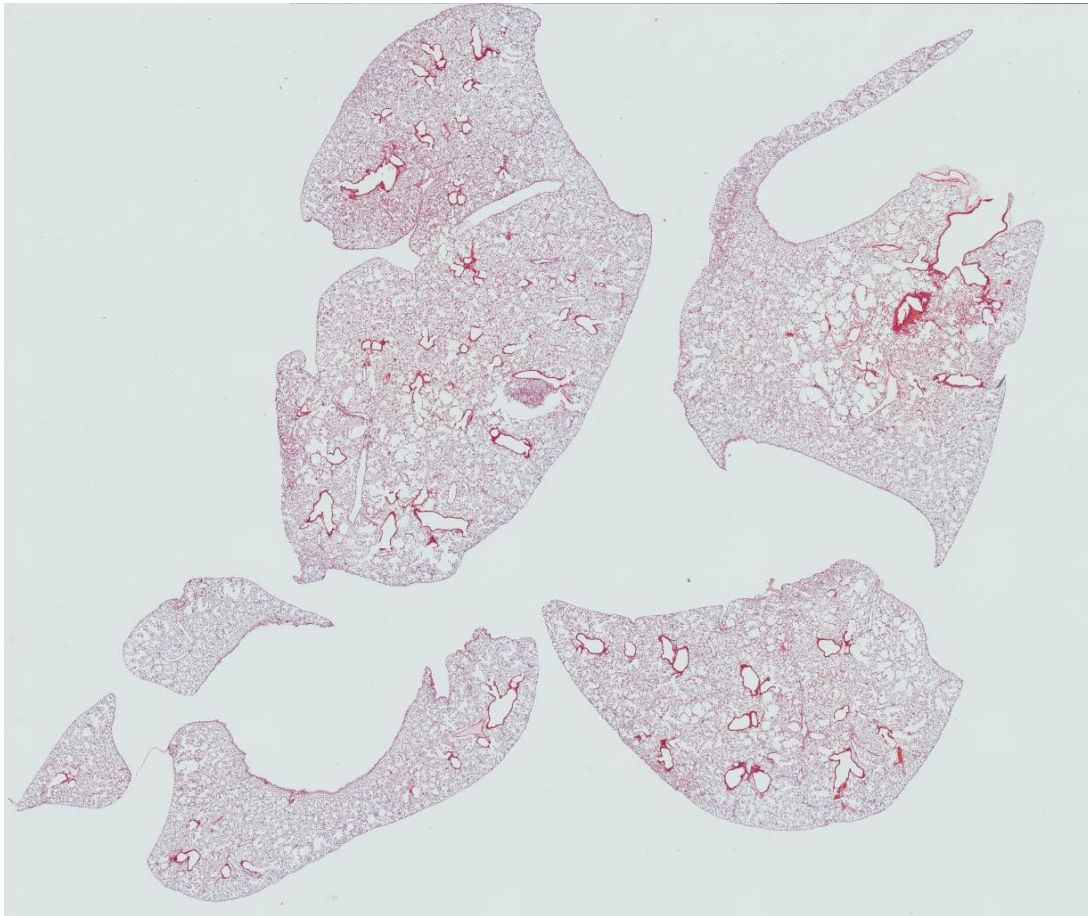
2446 WT 2.0 U

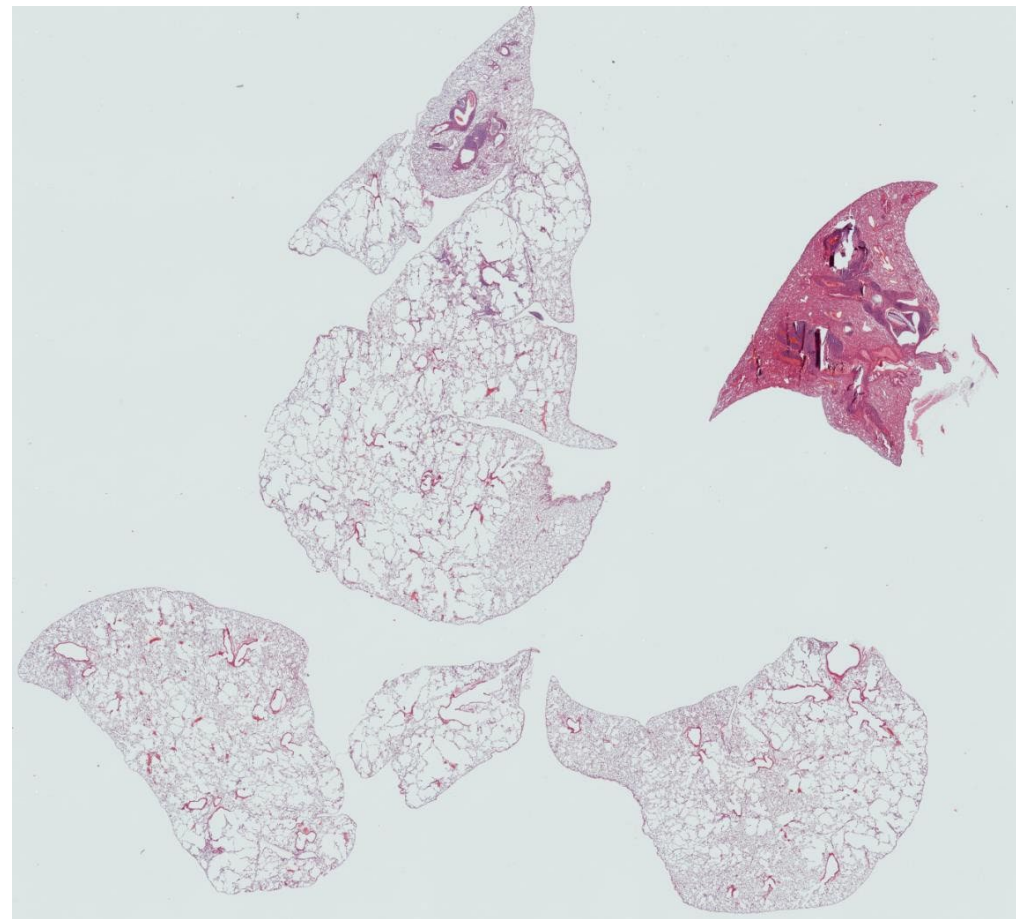


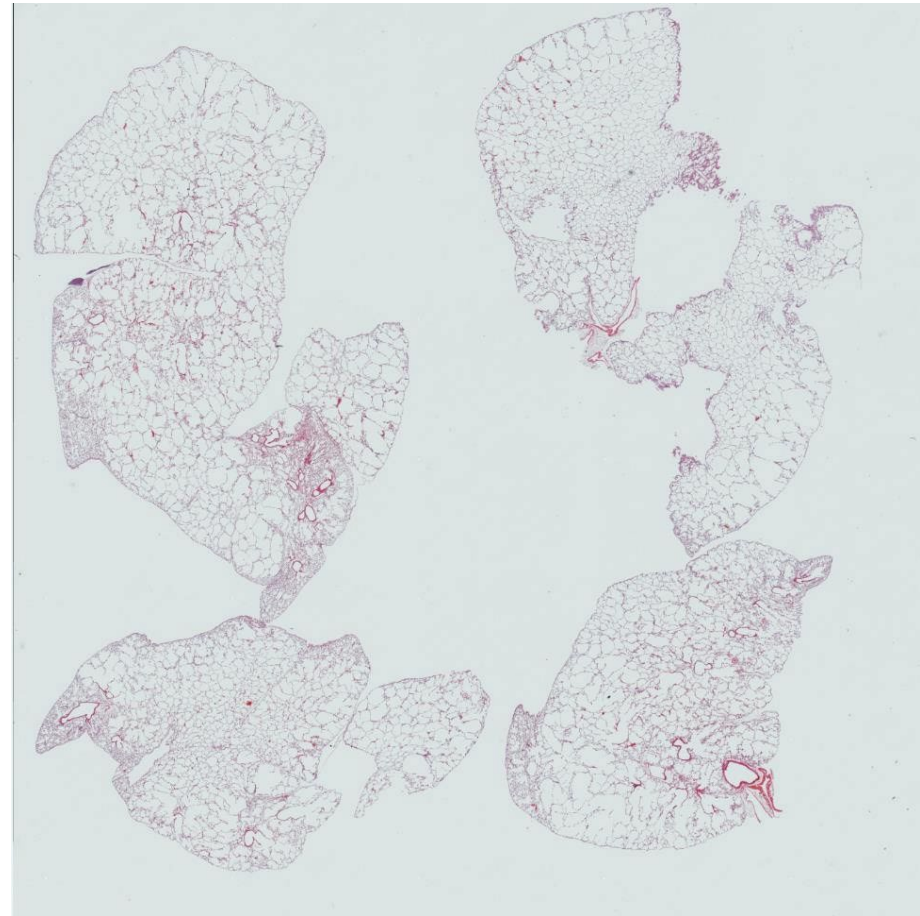
2456 WT 5.0 U



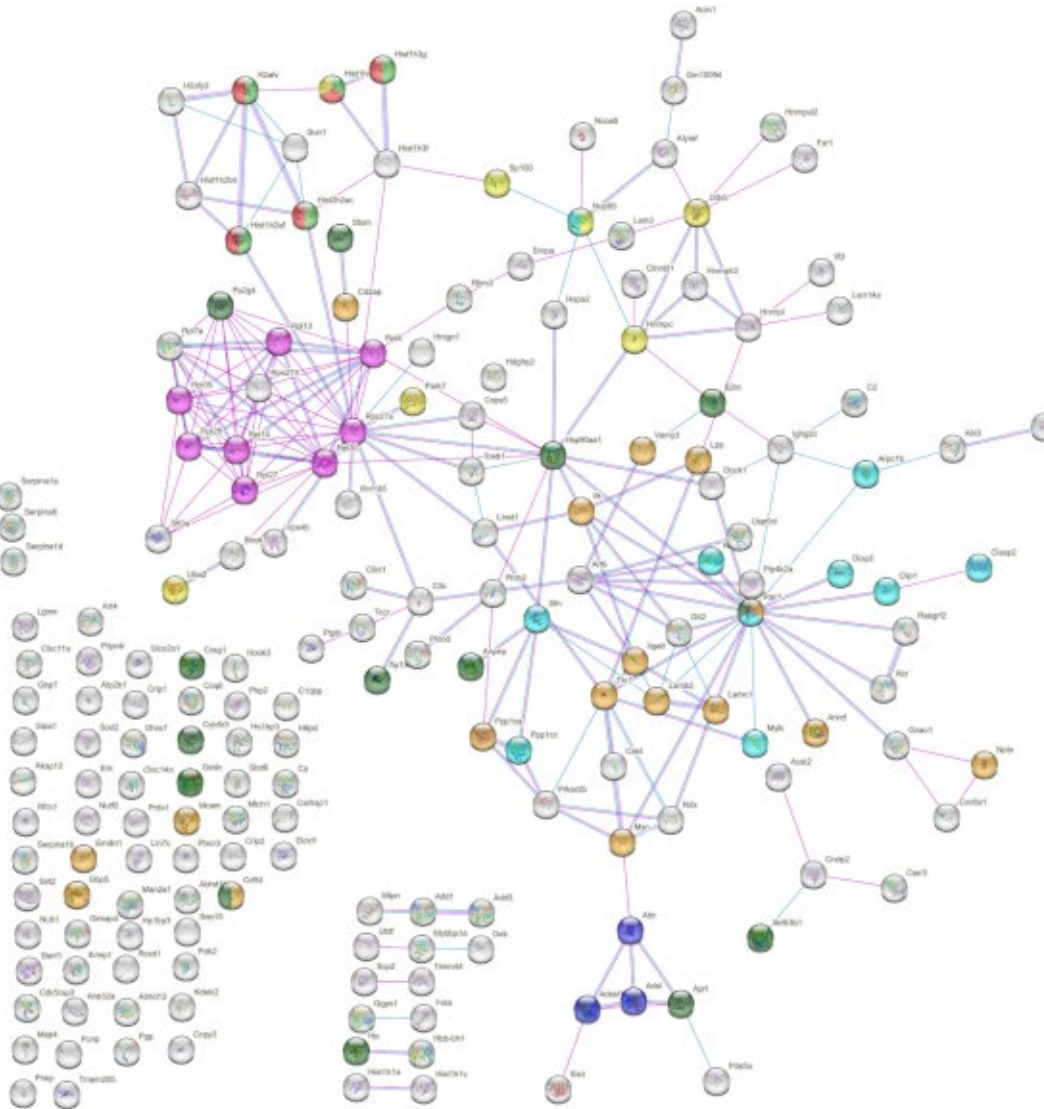
2445 WT 5.0 U





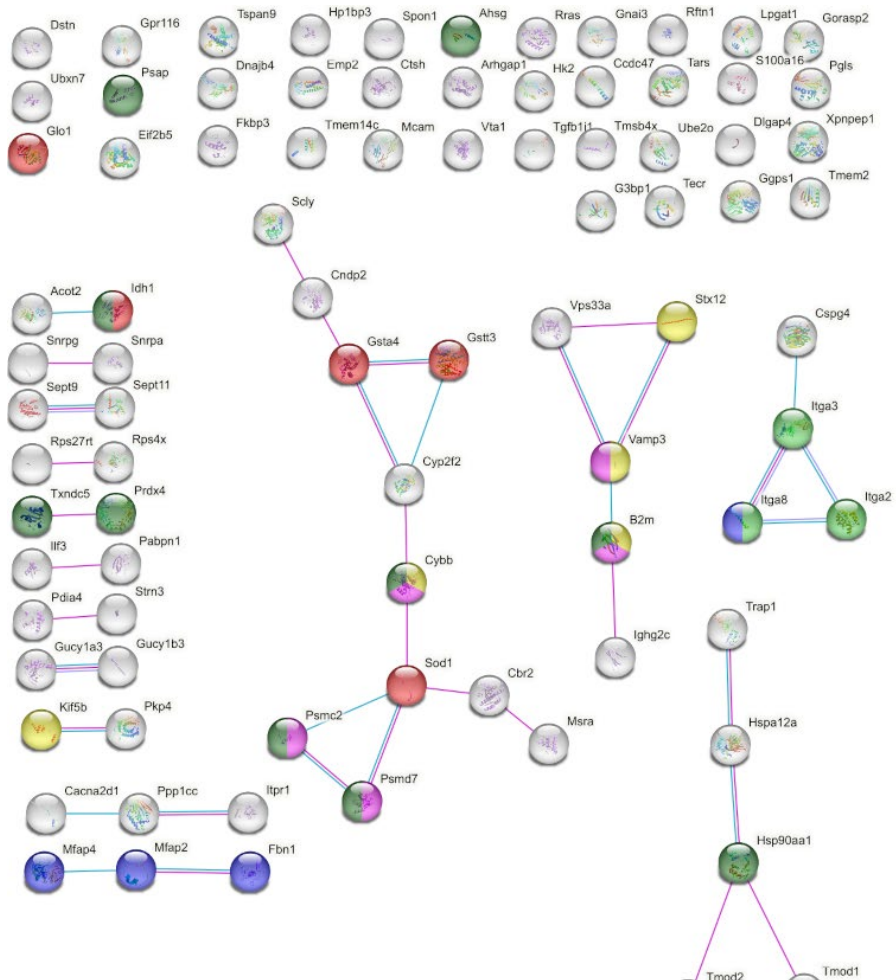


Supplemental Figure 3



pathway	description	count in network	strength	false discovery rate
MMU-73817	Purine ribonucleoside monophosphate biosynthesis	3 of 12	1.47	0.0095
MMU-110330	Recognition and association of DNA glycosylase with site c...	5 of 33	1.26	0.0016
MMU-9670095	Inhibition of DNA recombination at telomere	5 of 34	1.24	0.0017
MMU-110331	Cleavage of the damaged purine	5 of 35	1.23	0.0018
MMU-2297178	Condensation of Prophage Chromosomes	5 of 38	1.2	0.0019
MMU-212300	PRC2 methylates histones and DNA	5 of 40	1.17	0.0022
MMU-5689901	Metalloprotease DUBs	3 of 26	1.14	0.0493
MMU-1793339	SRP-dependent cotranslational protein targeting to membra...	9 of 88	1.09	0.00019
MMU-8936459	RUNX1 regulates genes involved in megakaryocyte different...	5 of 48	1.09	0.0041
MMU-7979956	Nonsense Mediated Decay (NMD) independent of the Exon _	9 of 90	1.08	0.00019
MMU-2559586	DNA Damage/Telomere Stress Induced Senescence	6 of 59	1.08	0.0017
MMU-212165	Epigenic regulation of gene expression	7 of 71	1.07	0.00034
MMU-3214858	RMT's methylate histone arginines	4 of 41	1.07	0.0191
MMU-72689	Formation of a pool of free 40S subunits	9 of 97	1.04	0.00019
MMU-737884	Base Excision Repair	6 of 70	1.01	0.0025
MMU-72706	GTP hydrolysis and joining of the 60S ribosomal subunit	9 of 108	1.0	0.00019
MMU-156827	L13a-mediated translational silencing of Ceruloplasmin exp...	9 of 107	1.0	0.00019
MMU-9795957	Nonsense Mediated Decay (NMD) enhanced by the Exon Ju...	9 of 110	0.99	0.00019
MMU-75153	Apoptotic execution phase	4 of 49	0.99	0.0214
MMU-6662729	Deposition of new CENPA-containing nucleosomes at the c...	4 of 52	0.96	0.0365
MMU-68875	Mitotic Prophase	7 of 96	0.94	0.0018
MMU-3214815	HDACs deacetylate histones	4 of 55	0.94	0.0428
MMU-6804834	Signaling by MET	5 of 78	0.88	0.0219
MMU-5357891	Programmed Cell Death	7 of 116	0.86	0.0041
MMU-2559583	Cellular Senescence	7 of 124	0.83	0.0055
MMU-6791226	Major pathway of rRNA processing in the nucleolus and cyl...	9 of 171	0.8	0.0018
MMU-2998046	SUMOylation	7 of 150	0.75	0.0136
MMU-72163	miRNA Splicing - Major Pathway	8 of 178	0.73	0.0073
MMU-5663220	RHO GTPases Activate Formins	6 of 133	0.73	0.0337
MMU-195258	RHO GTPase Effectors	10 of 246	0.69	0.0033
MMU-3108232	SUMO E3 Ligases SUMOylate target proteins	6 of 145	0.69	0.0478
MMU-68886	M Phase	14 of 364	0.66	0.00054
MMU-72203	Processing of Capped Intron-Containing Pre-mRNA	9 of 234	0.66	0.0086
MMU-2262752	Cellular responses to stress	14 of 395	0.63	0.0011
MMU-8938354	Metabolism of RNA	19 of 556	0.61	0.00019
MMU-1943175	Signaling by Rho GTPases	13 of 381	0.61	0.0019
MMU-622475	Axon guidance	9 of 278	0.59	0.0231
MMU-73894	DNA Repair	9 of 293	0.56	0.0314
MMU-6796695	Neutrophil degranulation	14 of 519	0.51	0.0069
MMU-1640170	Cell Cycle	15 of 574	0.49	0.0060
MMU-158249	Innate Immune System	21 of 949	0.42	0.0033
MMU-392499	Metabolism of proteins	27 of 1609	0.3	0.0181
MMU-1582356	Immune System	27 of 1621	0.3	0.0194
GO_0022410	Biological adhesion	17 of 731	0.49	0.0450
GO_0009735	Structural constituent of ribosome	8 of 185	0.39	0.0171

Supplemental Figure 4



pathway	description	count in network	strength	false discovery rate
MMU-2129379	Molecules associated with elastic fibres	4 of 35	1.47	0.0255
MMU-1236975	Antigen processing-Cross presentation	5 of 92	1.14	0.0255
MMU-6798695	Neutrophil degranulation	10 of 519	0.69	0.0255
GO-0006749	Glutathione metabolic process	5 of 53	1.38	0.0155
GO:0008305	Integrin complex	3 of 30	1.41	0.0301
GO_0045335	Phagocytic vesicle	5 of 112	1.06	0.0134